VALIDITY OF DARCY'S LAW FOR LOW-GRADIENT SATURATED FLOW THROUGH BENTONITE AND SAND MIXTURES

BY

THAYALAN KARTHIGESU

A Thesis
Submitted to the Faculty of Graduate Studies
in Partial Fulfilment of the Requirements for the Degree of

MASTER OF SCIENCE

Department of Agricultural Engineering
University of Manitoba
Winnipeg, Manitoba

National Library
of Canada

Acquisitions and
Bibliographic Services Branch

395 Wellington Street
Ottawa, Ontario
K1A 0N4

Bibliothèque nationale
du Canada

Direction des acquisitions et
des services bibliographiques

395, rue Wellington
Ottawa (Ontario)
K1A 0N4

Your file Votre référence

Our file Notre référence

ISBN 0-315-92297-4

Canada

Name ___

Dissertation Abstracts International is arranged by broad, general subject categories. Please select the one subject which most nearly describes the content of your dissertation. Enter the corresponding four-digit code in the spaces provided.

AGRICULTURAL ENGINEERING
SUBJECT TERM

0539
SUBJECT CODE

U·M·I

Subject Categories

THE HUMANITIES AND SOCIAL SCIENCES

COMMUNICATIONS AND THE ARTS
Architecture 0729
Art History 0377
Cinema 0900
Dance 0378
Fine Arts 0357
Information Science 0723
Journalism 0391
Library Science 0399
Mass Communications 0708
Music 0413
Speech Communication 0459
Theater 0465

EDUCATION
General 0515
Administration 0514
Adult and Continuing 0516
Agricultural 0517
Art 0273
Bilingual and Multicultural 0282
Business 0688
Community College 0275
Curriculum and Instruction 0727
Early Childhood 0518
Elementary 0524
Finance 0277
Guidance and Counseling 0519
Health 0680
Higher 0745
History of 0520
Home Economics 0278
Industrial 0521
Language and Literature 0279
Mathematics 0280
Music 0522
Philosophy of 0998
Physical 0523
Psychology 0525
Reading 0535
Religious 0527
Sciences 0714
Secondary 0533
Social Sciences 0534
Sociology of 0340
Special 0529
Teacher Training 0530
Technology 0710
Tests and Measurements 0288
Vocational 0747

LANGUAGE, LITERATURE AND LINGUISTICS
Language
- General 0679
- Ancient 0289
- Linguistics 0290
- Modern 0291

Literature
- General 0401
- Classical 0294
- Comparative 0295
- Medieval 0297
- Modern 0298
- African 0316
- American 0591
- Asian 0305
- Canadian (English) 0352
- Canadian (French) 0355
- English 0593
- Germanic 0311
- Latin American 0312
- Middle Eastern 0315
- Romance 0313
- Slavic and East European 0314

PHILOSOPHY, RELIGION AND THEOLOGY
Philosophy 0422
Religion
- General 0318
- Biblical Studies 0321
- Clergy 0319
- History of 0320
- Philosophy of 0322

Theology 0469

SOCIAL SCIENCES
American Studies 0323
Anthropology
- Archaeology 0324
- Cultural 0326
- Physical 0327

Business Administration
- General 0310
- Accounting 0272
- Banking 0770
- Management 0454
- Marketing 0338

Canadian Studies 0385
Economics
- General 0501
- Agricultural 0503
- Commerce-Business 0505
- Finance 0508
- History 0509
- Labor 0510
- Theory 0511

Folklore 0358
Geography 0366
Gerontology 0351
History
- General 0578
- Ancient 0579
- Medieval 0581
- Modern 0582
- Black 0328
- African 0331
- Asia, Australia and Oceania 0332
- Canadian 0334
- European 0335
- Latin American 0336
- Middle Eastern 0333
- United States 0337

History of Science 0585
Law 0398
Political Science
- General 0615
- International Law and Relations 0616
- Public Administration 0617

Recreation 0814
Social Work 0452
Sociology
- General 0626
- Criminology and Penology 0627
- Demography 0938
- Ethnic and Racial Studies 0631
- Individual and Family Studies 0628
- Industrial and Labor Relations 0629
- Public and Social Welfare 0630
- Social Structure and Development 0700
- Theory and Methods 0344

Transportation 0709
Urban and Regional Planning 0999
Women's Studies 0453

THE SCIENCES AND ENGINEERING

BIOLOGICAL SCIENCES
Agriculture
- General 0473
- Agronomy 0285
- Animal Culture and Nutrition 0475
- Animal Pathology 0476
- Food Science and Technology 0359
- Forestry and Wildlife 0478
- Plant Culture 0479
- Plant Pathology 0480
- Plant Physiology 0817
- Range Management 0777
- Wood Technology 0746

Biology
- General 0306
- Anatomy 0287
- Biostatistics 0308
- Botany 0309
- Cell 0379
- Ecology 0329
- Entomology 0353
- Genetics 0369
- Limnology 0793
- Microbiology 0410
- Molecular 0307
- Neuroscience 0317
- Oceanography 0416
- Physiology 0433
- Radiation 0821
- Veterinary Science 0778
- Zoology 0472

Biophysics
- General 0786
- Medical 0760

EARTH SCIENCES
Biogeochemistry 0425
Geochemistry 0996
Geodesy 0370
Geology 0372
Geophysics 0373
Hydrology 0388
Mineralogy 0411
Paleobotany 0345
Paleoecology 0426
Paleontology 0418
Paleozoology 0985
Palynology 0427
Physical Geography 0368
Physical Oceanography 0415

HEALTH AND ENVIRONMENTAL SCIENCES
Environmental Sciences 0768
Health Sciences
- General 0566
- Audiology 0300
- Chemotherapy 0992
- Dentistry 0567
- Education 0350
- Hospital Management 0769
- Human Development 0758
- Immunology 0982
- Medicine and Surgery 0564
- Mental Health 0347
- Nursing 0569
- Nutrition 0570
- Obstetrics and Gynecology 0380
- Occupational Health and Therapy 0354
- Ophthalmology 0381
- Pathology 0571
- Pharmacology 0419
- Pharmacy 0572
- Physical Therapy 0382
- Public Health 0573
- Radiology 0574
- Recreation 0575
- Speech Pathology 0460
- Toxicology 0383

Home Economics 0386

PHYSICAL SCIENCES
Pure Sciences
Chemistry
- General 0485
- Agricultural 0749
- Analytical 0486
- Biochemistry 0487
- Inorganic 0488
- Nuclear 0738
- Organic 0490
- Pharmaceutical 0491
- Physical 0494
- Polymer 0495
- Radiation 0754

Mathematics 0405
Physics
- General 0605
- Acoustics 0986
- Astronomy and Astrophysics 0606
- Atmospheric Science 0608
- Atomic 0748
- Electronics and Electricity 0607
- Elementary Particles and High Energy 0798
- Fluid and Plasma 0759
- Molecular 0609
- Nuclear 0610
- Optics 0752
- Radiation 0756
- Solid State 0611

Statistics 0463

Applied Sciences
Applied Mechanics 0346
Computer Science 0984
Engineering
- General 0537
- Aerospace 0538
- Agricultural 0539
- Automotive 0540
- Biomedical 0541
- Chemical 0542
- Civil 0543
- Electronics and Electrical 0544
- Heat and Thermodynamics 0348
- Hydraulic 0545
- Industrial 0546
- Marine 0547
- Materials Science 0794
- Mechanical 0548
- Metallurgy 0743
- Mining 0551
- Nuclear 0552
- Packaging 0549
- Petroleum 0765
- Sanitary and Municipal 0554
- System Science 0790

Geotechnology 0428
Operations Research 0796
Plastics Technology 0795
Textile Technology 0994

PSYCHOLOGY
General 0621
Behavioral 0384
Clinical 0622
Developmental 0620
Experimental 0623
Industrial 0624
Personality 0625
Physiological 0989
Psychobiology 0349
Psychometrics 0632
Social 0451

Nom _____

Dissertation Abstracts International est organisé en catégories de sujets. Veuillez s.v.p. choisir le sujet qui décrit le mieux votre thèse et inscrivez le code numérique approprié dans l'espace réservé ci-dessous.

_____ ☐☐☐ U·M·I

SUJET — CODE DE SUJET

Catégories par sujets

HUMANITÉS ET SCIENCES SOCIALES

COMMUNICATIONS ET LES ARTS
Architecture 0729
Beaux-arts 0357
Bibliothéconomie 0399
Cinéma 0900
Communication verbale 0459
Communications 0708
Danse 0378
Histoire de l'art 0377
Journalisme 0391
Musique 0413
Sciences de l'information 0723
Théâtre 0465

ÉDUCATION
Généralités 515
Administration 0514
Art 0273
Collèges communautaires 0275
Commerce 0688
Économie domestique 0278
Éducation permanente 0516
Éducation préscolaire 0518
Éducation sanitaire 0680
Enseignement agricole 0517
Enseignement bilingue et multiculturel 0282
Enseignement industriel 0521
Enseignement primaire. 0524
Enseignement professionnel 0747
Enseignement religieux 0527
Enseignement secondaire 0533
Enseignement spécial 0529
Enseignement supérieur 0745
Évaluation 0288
Finances 0277
Formation des enseignants 0530
Histoire de l'éducation 0520
Langues et littérature 0279
Lecture 0535
Mathématiques 0280
Musique 0522
Orientation et consultation 0519
Philosophie de l'éducation 0998
Physique 0523
Programmes d'études et enseignement 0727
Psychologie 0525
Sciences 0714
Sciences sociales 0534
Sociologie de l'éducation 0340
Technologie 0710

LANGUE, LITTÉRATURE ET LINGUISTIQUE
Langues
- Généralités 0679
- Anciennes 0289
- Linguistique 0290
- Modernes 0291

Littérature
- Généralités 0401
- Anciennes 0294
- Comparée 0295
- Médiévale 0297
- Moderne 0298
- Africaine 0316
- Américaine 0591
- Anglaise 0593
- Asiatique 0305
- Canadienne (Anglaise) 0352
- Canadienne (Française) 0355
- Germanique 0311
- Latino-américaine 0312
- Moyen-orientale 0315
- Romane 0313
- Slave et est-européenne 0314

PHILOSOPHIE, RELIGION ET THÉOLOGIE
Philosophie 0422
Religion
- Généralités 0318
- Clergé 0319
- Études bibliques 0321
- Histoire des religions 0320
- Philosophie de la religion 0322

Théologie 0469

SCIENCES SOCIALES
Anthropologie
- Archéologie 0324
- Culturelle 0326
- Physique 0327

Droit 0398
Économie
- Généralités 0501
- Commerce-Affaires 0505
- Économie agricole 0503
- Économie du travail 0510
- Finances 0508
- Histoire 0509
- Théorie 0511

Études américaines 0323
Études canadiennes 0385
Études féministes 0453
Folklore 0358
Géographie 0366
Gérontologie 0351
Gestion des affaires
- Généralités 0310
- Administration 0454
- Banques 0770
- Comptabilité 0272
- Marketing 0338

Histoire
- Histoire générale 0578
- Ancienne 0579
- Médiévale 0581
- Moderne 0582
- Histoire des noirs 0328
- Africaine 0331
- Canadienne 0334
- États-Unis 0337
- Européenne 0335
- Moyen-orientale 0333
- Latino-américaine 0336
- Asie, Australie et Océanie 0332

Histoire des sciences 0585
Loisirs 0814
Planification urbaine et régionale 0999
Science politique
- Généralités 0615
- Administration publique 0617
- Droit et relations internationales 0616

Sociologie
- Généralités 0626
- Aide et bien-être social 0630
- Criminologie et établissements pénitentiaires 0627
- Démographie 0938
- Études de l' individu et de la famille 0628
- Études des relations interethniques et des relations raciales 0631
- Structure et développement social 0700
- Théorie et méthodes. 0344
- Travail et relations industrielles 0629

Transports 0709
Travail social 0452

SCIENCES ET INGÉNIERIE

SCIENCES BIOLOGIQUES
Agriculture
- Généralités 0473
- Agronomie. 0285
- Alimentation et technologie alimentaire 0359
- Culture 0479
- Élevage et alimentation 0475
- Exploitation des pâturages 0777
- Pathologie animale 0476
- Pathologie végétale 0480
- Physiologie végétale 0817
- Sylviculture et faune 0478
- Technologie du bois 0746

Biologie
- Généralités 0306
- Anatomie 0287
- Biologie (Statistiques) 0308
- Biologie moléculaire 0307
- Botanique 0309
- Cellule 0379
- Écologie 0329
- Entomologie 0353
- Génétique 0369
- Limnologie 0793
- Microbiologie 0410
- Neurologie 0317
- Océanographie 0416
- Physiologie 0433
- Radiation 0821
- Science vétérinaire 0778
- Zoologie 0472

Biophysique
- Généralités 0786
- Medicale 0760

SCIENCES DE LA TERRE
Biogéochimie 0425
Géochimie 0996
Géodésie 0370
Géographie physique 0368
Géologie 0372
Géophysique 0373
Hydrologie 0388
Minéralogie 0411
Océanographie physique 0415
Paléobotanique 0345
Paléoécologie 0426
Paléontologie 0418
Paléozoologie 0985
Palynologie 0427

SCIENCES DE LA SANTÉ ET DE L'ENVIRONNEMENT
Économie domestique 0386
Sciences de l'environnement 0768
Sciences de la santé
- Généralités 0566
- Administration des hôpitaux 0769
- Alimentation et nutrition 0570
- Audiologie 0300
- Chimiothérapie 0992
- Dentisterie 0567
- Développement humain 0758
- Enseignement 0350
- Immunologie 0982
- Loisirs 0575
- Médecine du travail et thérapie 0354
- Médecine et chirurgie 0564
- Obstétrique et gynécologie 0380
- Ophtalmologie 0381
- Orthophonie 0460
- Pathologie 0571
- Pharmacie 0572
- Pharmacologie 0419
- Physiothérapie 0382
- Radiologie 0574
- Santé mentale 0347
- Santé publique 0573
- Soins infirmiers 0569
- Toxicologie 0383

SCIENCES PHYSIQUES
Sciences Pures
Chimie
- Généralités 0485
- Biochimie 487
- Chimie agricole 0749
- Chimie analytique 0486
- Chimie minérale 0488
- Chimie nucléaire 0738
- Chimie organique 0490
- Chimie pharmaceutique 0491
- Physique 0494
- PolymÈres 0495
- Radiation 0754

Mathématiques 0405
Physique
- Généralités 0605
- Acoustique 0986
- Astronomie et astrophysique 0606
- Électronique et électricité 0607
- Fluides et plasma 0759
- Météorologie 0608
- Optique 0752
- Particules (Physique nucléaire) 0798
- Physique atomique 0748
- Physique de l'état solide 0611
- Physique moléculaire 0609
- Physique nucléaire 0610
- Radiation 0756

Statistiques 0463

Sciences Appliqués Et Technologie
Informatique 0984
Ingénierie
- Généralités 0537
- Agricole 0539
- Automobile 0540
- Biomédicale 0541
- Chaleur et thermodynamique 0348
- Conditionnement (Emballage) 0549
- Génie aérospatial 0538
- Génie chimique 0542
- Génie civil 0543
- Génie électronique et électrique 0544
- Génie industriel 0546
- Génie mécanique 0548
- Génie nucléaire 0552
- Ingénierie des systèmes 0790
- Mécanique navale 0547
- Métallurgie 0743
- Science des matériaux 0794
- Technique du pétrole 0765
- Technique minière 0551
- Techniques sanitaires et municipales 0554
- Technologie hydraulique 0545

Mécanique appliquée 0346
Géotechnologie 0428
Matières plastiques (Technologie) 0795
Recherche opérationnelle 0796
Textiles et tissus (Technologie) 0794

PSYCHOLOGIE
Généralités 0621
Personnalité 0625
Psychobiologie 0349
Psychologie clinique 0622
Psychologie du comportement 0384
Psychologie du développement 0620
Psychologie expérimentale 0623
Psychologie industrielle 0624
Psychologie physiologique 0989
Psychologie sociale 0451
Psychométrie 0632

VALIDITY OF DARCY'S LAW FOR LOW-GRADIENT SATURATED FLOW THROUGH BENTONITE AND SAND MIXTURES

BY

THAYALAN KARTHIGESU

A Thesis submitted to the Faculty of Graduate Studies of the University of Manitoba in partial fulfillment of the requirements for the degree of

MASTER OF SCIENCE

Abstract

Published data on hydraulic flow through saturated clays show deviations from the linear relationship of Darcy's law. Experimental errors in some studies are of sufficient magnitude to account for the deviations. Errors associated with conventional instrumentation make it difficult to measure the flow rate accurately under low hydraulic gradients. Precise measurement of flow velocities under very low hydraulic gradients becomes very important for testing the validity of Darcy's law in this range of hydraulic gradient.

An improved technique, employing a liquid bubble flow meter, is used for testing five-percent and ten-percent Na-bentonite and sand mixtures under low hydraulic gradients. Na-bentonite was selected for this study since soil and bentonite mixes are frequently used as impervious liners for waste disposal facilities. The equipment and testing procedures of this improved technique are described. The results show a lower saturated hydraulic conductivity at hydraulic gradients less than four when compared to the values obtained in the higher range.

A model based on a modified flow equation is proposed to account for the nonlinear behaviour in the lower range of hydraulic gradient. The model was validated using data obtained in the laboratory.

Acknowledgements

The author wishes to acknowledge with gratitude the assistance of his advisor, Dr. R. Sri Ranjan whose ideas, enthusiasm, encouragement and time have contributed immensely to this study. A most hearty "thank you" is extended to him.

Sincere appreciation is extended to Dr. G. E. Laliberte for his encouragement and advice during the various stages of the research program.

The author appreciates the assistance of Dr. N. R. Bulley for his guidance and suggestions in the initial stages of this project.

A special word of thanks is extended to Dr. C. M. Cho for his encouragement and assistance particularly in the development of the modified flow model equations.

The author would like to thank Mr. Jack Putnam, Mr. Jim Philp, Mr. Matt McDonald and Mr. Rob Attaman for the excellent technical support in setting up the experiment.

The financial support from the Natural Sciences and Engineering Research Council of Canada is acknowledged.

Table of Contents

List of Figures

List of Tables

1. Introduction

1.1 Scope

Groundwater contamination has become a major concern in recent years due to increased production and improper disposal of chemical and radioactive wastes. Low permeability and low diffusion coefficients of clays make them an ideal barrier material to prevent hazardous contaminants from entering groundwater regimes. Permeability is also a key element in foundation engineering and design of water-retaining structures.

Generally, two transport mechanisms can be distinguished in clays, that is, diffusion and flow. Concentration gradient is the propelling force for diffusion. In soils, water flows in response to hydraulic, osmotic and thermal gradients. Even though subsurface migration of hazardous wastes is primarily controlled by the permeability of soil, it has not been investigated as intensively as their mechanical behaviour (Tavenas et al., 1983).

Validity of the classic equation relating flow velocity to hydraulic gradient, Darcy's law, is not clearly established for low-hydraulic-gradient flows. When the advective component (flow due to hydraulic gradient) of flow is low, a molecular diffusion mechanism controls the solute transport (Cherry et al., 1984, Hasenpatt et al., 1989, Shackleford et al., 1989, Sri Ranjan and Gillham, 1991). A clear understanding of flow under low hydraulic gradients is needed to determine the relative importance of diffusion and other flow mechanisms involved under such conditions. Precise measurement of flow velocities under very low hydraulic gradients becomes critically important for checking the validity of Darcy's law under such conditions.

Several investigators have published data that show hydraulic flow through saturated clays deviates from Darcy's law. An error due to atmospheric contamination in conventional flow meters that use air-water menisci or air bubbles in capillary tubes may have been overlooked in previous studies. Olsen (1965) has shown that the contamination error is of sufficient magnitude to account for the observed deviations in much of the published data on confined clays. Olsen (1965) used a constant-flow-rate syringe pump to avoid errors arising from atmospheric contamination. The capability of the pump used by Olsen (1965) is limited by the slowest obtainable flux (1.23×10^{-8} m s^{-1}).

In the present study, an improved technique using a liquid bubble flow meter is used in testing saturated Na-bentonite and sand mixtures. The inflow rate and outflow rate were measured separately. Only the outflow values were analyzed as they represent the actual amount of water passing through the samples. The inflow was used as a guide in determining when equilibrium had been reached. This system is capable of measuring flux down to 10^{-12} m s^{-1}.

Two sets of five-percent and ten-percent Na-bentonite (by weight) and sand (Selkirk silica sand - 150-200-μm-diameter) mixtures were packed in 70-mm-inside-diameter sample holders. Each set had three samples. In each sample, eight repetitive measurements were taken for each increment in hydraulic gradient.

Non-linear low-hydraulic-gradient flow behaviour was observed in both five-percent and ten-percent Na-bentonite and sand mixtures. The log-log plot of flux

as a function of hydraulic gradient on five-percent and ten-percent samples shows a change in slope in the one to four hydraulic gradient range. If Darcy's linear flow equation is used to model the flow, the flux as a function of hydraulic gradient relationship should go through the origin, in a linear plot.

A modified flow equation is proposed to model the non-linear flow behaviour under saturated conditions. In capillary flow, the fluid viscosity is assumed to be the same in the entire cross section. The modified flow equation for low-hydraulic-gradient flow through clays has two components; that is, flow through structured water with a higher viscosity (μ^{II}), and flow with the normal viscosity (μ^{I}). The proposed model assumes a gradual increase in the effective cross sectional area of lower-viscosity fluid flow with increasing hydraulic gradient across the sample. The flux as a function of hydraulic gradient relationships for the Na-bentonite and sand mixtures was simulated by both a spreadsheet package and a Fortran program, using the modified flow equation.

When measurements were completed, the samples were removed, filled with water in the outflow and inflow tubes, wrapped in an aluminum foil and kept for further testing. Tests on these samples will be used to show the effect of long-term storage on the saturated hydraulic conductivity of this clay. The usage of hydraulic conductivity values obtained from samples, tested under higher hydraulic gradients, may tend to over-estimate the flow rates under low hydraulic gradients. Different types of clays have to be tested to generalize the low-hydraulic-gradient flow behaviour and validate the proposed modified flow model for other clays.

1.2 Objectives

The main objectives of this thesis project were,

1) to determine flow as a function of hydraulic gradient relationship in saturated sand-bentonite mixtures using an improved liquid bubble flow meter at low hydraulic gradients,

2) to check the validity of Darcy's law under low hydraulic gradients,

3) to model the flow behaviour and evaluate it with laboratory flow measurements.

2 Review of Literature

2.1 Darcy's law

D'Arcy (1856) measured the flow of water through a vertical column of sand packed in a 2.5-m-long 0.35-mm-inside-diameter pipe. He found that the discharge rate expressed as volume of water flow per second per square meter is directly proportional to the head difference and inversely proportional to the length of the sample (Equation 2.1).

$$\frac{Q}{A} \propto \frac{-\Delta h}{L} \qquad [2.1]$$

where,

Q = volume of water flow per unit time (m^3 s^{-1})

A = cross sectional area (m^2)

L = length of the sample (m)

Δh = head difference (m)

But

$$q = Q / A \qquad [2.2]$$

and

$$i = \frac{\Delta h}{L} \qquad [2.3]$$

where,

q = macroscopic flow velocity (flux) (m s^{-1})

i = hydraulic gradient (m m^{-1})

From Equations 2.1, 2.2 and 2.3,

$$q \propto -i \qquad [2.4]$$

From Equation 2.4,

$$q = -Ki \qquad [2.5]$$

where,

K = saturated hydraulic conductivity (m s^{-1})

Intrinsic permeability depends only on the characteristics of the soil while the hydraulic conductivity depends on both the fluid and the soil characteristics as shown below.

$$K = \frac{k\rho g}{\mu} \qquad [2.6]$$

where,

k = intrinsic permeability (m^2)

μ = dynamic viscosity of the fluid (Pa s^{-1})

ρ = fluid density (kg m^{-3})

g = gravitational acceleration (m s^{-2})

The saturated hydraulic conductivities of different types of soil are typically within the ranges shown in Table 2.1. Hydraulic conductivity decreases with decreasing particle size. Crude estimates of saturated hydraulic conductivity can be made from particle size distribution.

TABLE 2.1 Saturated hydraulic conductivities of different soils (Craig, 1974)

Hydraulic conductivity										
m s^{-1}										
10^{-2}	10^{-3}	10^{-4}	10^{-5}	10^{-6}	10^{-7}	10^{-8}	10^{-9}	10^{-10}	10^{-11}	10^{-12}
clean gravel gravel		clean sand and sand gravel mixtures			very fine sands and clay silt			clays and clay silts (>20% clay)		

2.2 Conventional measurement

The conventional laboratory technique for determining the hydraulic conductivity of saturated clays consists essentially of :

1) placing a clay sample in a test cell connected in series with a capillary tube containing an air-water meniscus or an air bubble;

2) producing flow through the clay with a known hydraulic head difference across the test cell-capillary tube system; and

3) determining the induced flow rate from measurements of the rate at which the meniscus or air bubble moves through the capillary tube (Olsen, 1966).

The head difference across the clay sample itself is determined by correcting the applied head difference for the pressure changes across the menisci in the capillary tube. Corrections are calculated from the theory of capillarity using handbook values for the surface tension of an air water meniscus and for the contact angle θ of water on glass (Olsen, 1965).

2.2.1 Contact angle

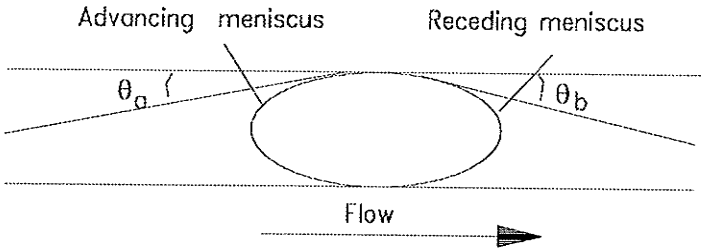

Figure 2.1 Advancing and receding menisci

Conventionally, the hydraulic characteristics of saturated clay samples are measured with an apparatus that consists of a test cell connected in series with a capillary tube. Flow rates are measured by the movement of either an air-permeant meniscus or air bubble through the tubes. Air bubbles in cylindrical capillary tubes can support finite differences in pressure (Smith and Crane, 1930). When contamination is present, the difference in head is shared by the air bubble and the clay sample placed in series. The head difference across an air bubble equals zero because the pressure differences across opposing ideal menisci of 0° contact angle cancel each other. An error occurs in the above procedure as liquid and solid surfaces are nearly always contaminated

by trace amounts of grease adsorbed from the atmosphere and from valve joints and other fittings.

The contact angle of water on contaminated glass does not equal the handbook value of 0°. It varies between a maximum of θ_a, for an advancing meniscus and a minimum of θ_b, for a receding meniscus (Figure 2.1). The difference between θ_a and θ_b , known as hysteresis, causes a head difference across opposing menisci. Experimentally measured contact-angles of water on contaminated mineral surfaces vary from 13° to 58° for receding menisci and from 62° to 90° for advancing menisci (Adam, 1941). Hysteresis values of 40° or more have been commonly observed (Adam, 1941).

Smith and Crane (1930) described the hysteresis of the contact angle due to contamination by the following equation:

$$\Delta P_B = \frac{4}{d}\sigma(\cos\ \theta_b - \cos\ \theta_a) \qquad [2.7]$$

where,

ΔP_B = pressure difference across an air bubble (N m^{-2})

d = capillary tube diameter (m)

σ = surface tension of the air water interface (N m^{-1})

(for air water interface 0.072 N m^{-1} at 25°C)

θ_a = contact angle of the advancing meniscus in °

θ_b = contact angle of the receding meniscus in °

But

$$\Delta P_B = \rho g \Delta h_B \qquad [2.8]$$

where,

Δh_B = corresponding difference in hydraulic head (m)

ρ = density of the liquid (kg m^{-3}) (for water, 1000 kg m^{-3})

g = gravitational acceleration (m s^{-2}) (9.8 m s^{-2})

From Equations 2.7 and 2.8,

$$\Delta h_B = \frac{4}{\rho g d}\sigma(\cos\theta_a - \cos\theta_b) \qquad [2.9]$$

As an example, the pressure head across an air bubble with an advancing meniscus of 60° and a receding meniscus of 20°, in a 0.5-mm-inside-diameter capillary tube, calculated from Equation 2.9, was found to be 25.8 mm of water.

2.2.2 Surface tension

Interfacial force or surface tension σ, is determined by the chemical properties of two phases that are in contact, especially the chemical properties of the boundary layer of the two phases. The interfacial force at solid surfaces is important, because it controls which fluid is the wetting fluid and which is the non-wetting fluid. Almost any organic contaminant reduces the surface tension of pure water. Contamination reduces surface tension of an air-water interface. Surface tension of distilled water was found to be 0.060 N m^{-1}, 17 percent less than the handbook value of 0.072 N m^{-1} at 25°C (Olsen, 1965).

Contamination effects discussed in the above two sections are for air bubbles in capillary tubes. A liquid bubble which has self-cleaning ability is used in this study to minimize the contamination effects. Some adsorbed organic molecules, however, are very difficult to remove except by burning (Corey, 1990). Therefore, when measurements are complete on a sample, the glass inflow-outflow capillary tube system must be removed

and kept in a high-temperature oven (550°C) for 20 minutes and allowed to cool overnight.

2.2.3 Constant-flow-rate pump method

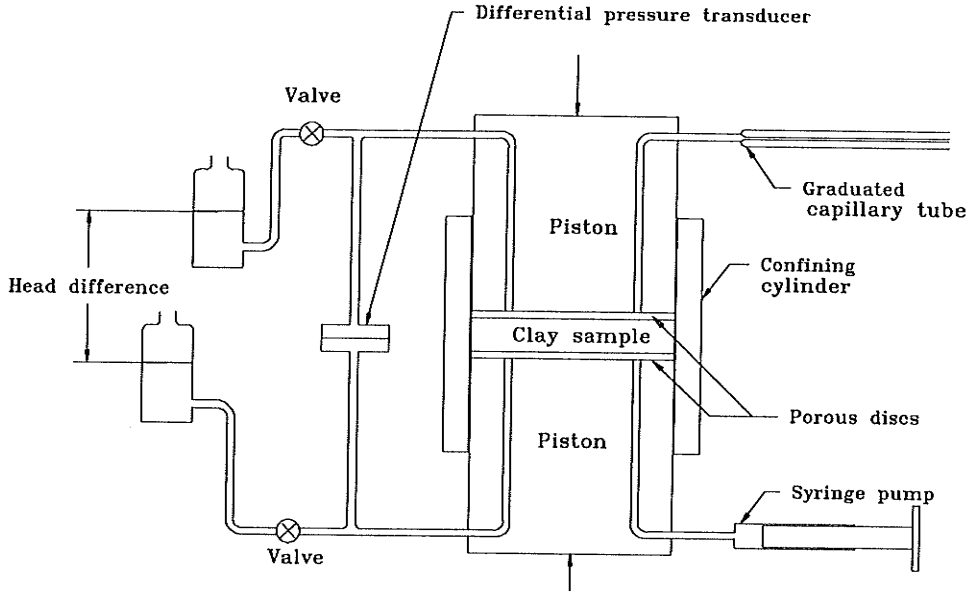

FIGURE 2.2 Constant-flow-rate pump method

Olsen (1966) used a new technique to investigate the validity of Darcy's law at low hydraulic gradients. In his study, samples of kaolinite were consolidated over a wide range of porosities. The essential difference from the conventional technique was that a known flow rate through the saturated clay sample was permitted, while the head differences induced across the sample by the applied flow rates were measured with a differential pressure transducer. The flow produced by the syringe pump passed through the clay sample either from the syringe to the capillary tube or in the reverse direction, where the liquid terminated in a meniscus.

The capability of this apparatus (Figure 2.2) was limited by the lowest flow rate obtainable with the syringe pump. The syringe barrel was glass and, therefore, experiments could be run only with permeant pressures in the order of atmospheric pressure. The lowest flow rate obtained, 10^{-12} m^3 s^{-1} , was one order of magnitude less than the flow rate used in previous experiments using capillary tubes. Olsen (1965) observed that lower flow rates would be needed to investigate the validity of Darcy's law at low hydraulic gradients in extremely fine-grained clays, particularly montmorillonite.

2.3 Types of deviations from Darcy's law

Non-Darcian flow behaviour is generally defined in terms of deviations from direct proportionality in the relationship between flow rate and hydraulic gradient.

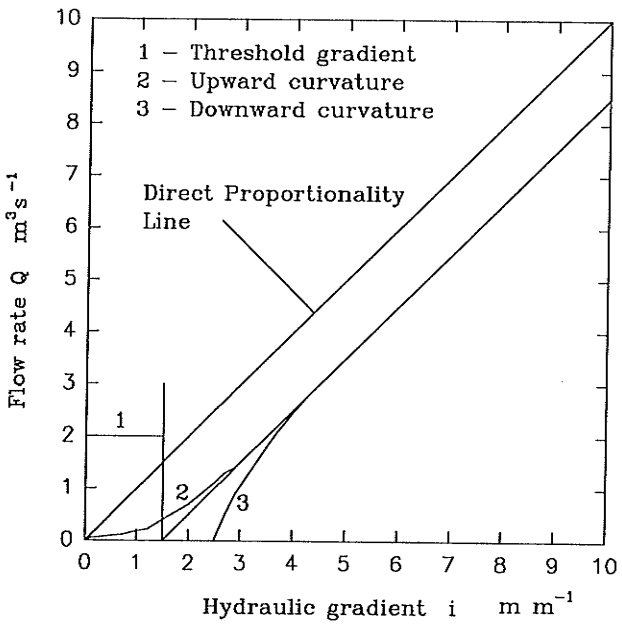

FIGURE 2.3 Relationships between volumetric flow rate and applied hydraulic gradient in porous materials showing deviations from Darcian flow

Reported deviations include both intercepts and curvatures (Figure 2.3):

i) a threshold gradient that must be exceeded before flow occurs;

ii) upward curvature where the hydraulic conductivity increases with increasing hydraulic gradient; and

iii) downward curvature where the hydraulic conductivity decreases with increasing hydraulic gradient.

2.3.1 Published deviations

Published deviations observed before 1965 are summarized in Table 2.2. The characteristics of Lutz and Kemper's (1959) samples of montmorillonite and halloysite and those of Von-Englehardt and Tunn's (1955) samples of sandstone that contained less than five percent clays were similar in two respects. First, the hydraulic gradients used, were as high as 500 and second, the clay samples were unconfined during the testing. Lack of confinement and large applied hydraulic gradients are favourable for the occurrence of deviations due to fabric changes caused by seepage. These results show that deviations from Darcy's law can occur due to alterations in the clay fabric when the system is unconfined.

Hansbo (1960) observed deviations on confined samples of natural illitic clays that were tested at hydraulic gradients ranging from one to four. These hydraulic gradients were in the order of those in the experiments conducted by Olsen in 1965. Olsen showed that all the deviations that Hansbo (1960) observed could be attributed to the contamination error in the conventional measurement technique.

TABLE 2.2 Deviations from Darcy's law summarized by Olsen (1966)

Name	Samples	Hydraulic Gradient	Flow meter	Type of observed deviations (Fig. 2.3)	Possible deviations (Olsen, (1966)
Von Englehardt and Tunn, 1955 (Unconfined)	Sandstone <5%clay	0-500	Single receding meniscus	2	0-1
Lutz and Kemper,1959 (Unconfined)	Montmori-llonite, Halloysite	0-500	Single receding meniscus	2,3	0-2
Hansbo, 1960 (Confined)	Illites	1-10	Air bubble in capillary	2	0-2.5
Li, 1963 (Confined)	Houston clay		Single oil-water menisci	1 *TG, 42	
Miller and Low, 1963 (Confined)	Montmori-llonite	0-100	Air bubble in graduated capillary tube	1,3 *TG, 8.8	0-10

*TG- Threshold Gradient

Miller and Low (1963) observed deviations in confined samples of montmorillonite over low and high ranges of hydraulic gradient. Olsen showed that part of the deviations was attributable to the contamination error. Slippage of liquid around the flow-rate-measuring air bubble can also lead to errors in the measurement. Miller and Low (1963) and Li (1963) confirmed the existence of threshold gradients in clays. Contamination also can cause an initial or threshold gradient to the flow through the capillary tubes and, therefore, precise measurement of low flow rates can become critically important to determine the cause of the observed initial hydraulic gradient.

In soils that consist partly or wholly of clay, liquid moves not only in response to hydraulic gradients, as described by Darcy's law, but also in response to osmotic and thermal gradients. These aspects were not considered in the studies carried out prior to 1965.

The hydraulic conductivity of quartz sand for boiled deionized water at room temperature was found to decrease markedly during prolonged flow (Gupta and Swartzendruber, 1962). A characteristic distribution of bacteria was found, consisting of a high number at the inlet end and a much lower number in the rest of the cell (Gupta and Swartzendruber, 1962).

Effective saturation is one of the factors affecting the permeability of porous media. Adam (1967) studied the diffusion of entrapped gas from porous media by measuring the weight gain as a function of time with samples of alundum (a ceramic material), diatomaceous earth and a variety of sandstones. Diffusion began as soon as the wetting front entered the sample and, as it advanced, some gas was able to leave the sample by bulk flow. Regardless of the material, the sample gained weight rapidly at the beginning of the measured time and the rate of gain decreased as time increased. Diatomaceous earth samples with porosity values in the range of 0.610 to 0.625 took 502 to 529 hours for complete saturation.

Abnormal water properties, electrokinetic coupling, fabric changes under the action of seepage forces and experimental errors are considered as possible causes for deviations from Darcy's law during hydraulic flow through fine-grained soils. Deviations from Darcy's law were observed in saturated kaolinite and in saturated compacted silty clay (Mitchell and Younger, 1967).

Deviations from Darcian proportionality between flow velocity and hydraulic gradient were considered in terms of a gradient-dependent hydraulic conductivity. Hydraulic conductivity K takes on a minimum value K_{min} at a hydraulic gradient i=0, and increases to a maximum value K_{max} as hydraulic gradient becomes large. The gradient-dependent velocity v was expressed by the following equation (Swartzendruber, 1968):

$$v = B[\ i\ - J\ (\ 1\ - e^{-Ci})\ ] \qquad [2.10]$$

where B, J and C are constants. Then

$$K_{max}\ /\ K_{min}\ = 1/\ (1\ - JC) \qquad [2.11]$$

In naturally occurring ground water systems, hydraulic gradients are generally one or less. Higher hydraulic gradients often exist across seepage blankets or compacted soil liners but they are unlikely to exceed 10 or 20 in most cases. However, in laboratory tests, hydraulic gradients of 150 to 200 are used for reasons of speed and economy. High hydraulic gradients may induce migration of soil particles, with resulting clogging of pore spaces or erosion of sample material. Hydraulic conductivity measurements were carried out by Dunn and Mitchell (1984) in two silty clay soils, Altamont soil and Rockville soil. These soils were compacted by static, impact and kneading methods of compaction. Hydraulic conductivity decreased with increasing hydraulic gradient in the range of 40 to 200 and the decrease was found to be irreversible with decreasing hydraulic gradient (Dunn and Mitchell, 1984).

2.3.2 A recent study on deviations from Darcy's law in bentonite and sand mixtures

In bentonite and sand mixtures, the bentonite is present in the pores between the sand particles. The pore water is adsorbed by the bentonite particles and the water molecules are adsorbed more strongly the closer they are to the clay surface. Therefore, the binding forces increase with increasing bentonite content in the pores. The binding of water molecules is so strong in bentonite liners that the hydraulic gradient needs to be quite high before all water molecules can move freely and obey Darcy's law (Hoeks et al., 1987). Gödecke (1980) reported that, in the low non-Darcian hydraulic gradient range, the flux is related to the hydraulic gradient by a power relation:

$$q = K_m i^{m} \qquad [2.12]$$

where,

K_m = saturated hydraulic conductivity at hydraulic gradient equal to one (m s^{-1})

m = constant

i = hydraulic gradient (m m^{-1})

The measured flow through mixtures of medium fine sand with five percent (by weight) of Wyoming bentonite showed a non-linear relationship with the imposed hydraulic gradient. Successive runs on the same sample showed that the hydraulic conductivity decreased with time. Hoeks et al. (1987) described the combined effect of time and hydraulic gradient on the flux in an equation:

$$q = (a_0 e^{-\alpha t} + a_f) i^{m} \qquad [2.13]$$

where,

a_o = constant (m s^{-1})

a_f = constant (m s^{-1})

α = constant (d^{-1})

m = constant

t = time since the start (d)

The constants a_0 and a_f depended on the bentonite content, the bentonite type and the soil type. For the mixtures tested by Hoeks et al. (1987) , the constants had the following values:

$a_0 = 1.1 \times 10^{-10}$ m s^{-1}

$a_f = 1.0 \times 10^{-10}$ m s^{-1}

$\alpha = 0.06\ d^{-1}$

m = 1.4

This non-Darcian flow can be very important, especially in swelling clays where Darcian flow may be reached only for hydraulic gradients in the range of 50-100 (Hoeks et al., 1987).

2.3.3 Viscosity of adsorbed water

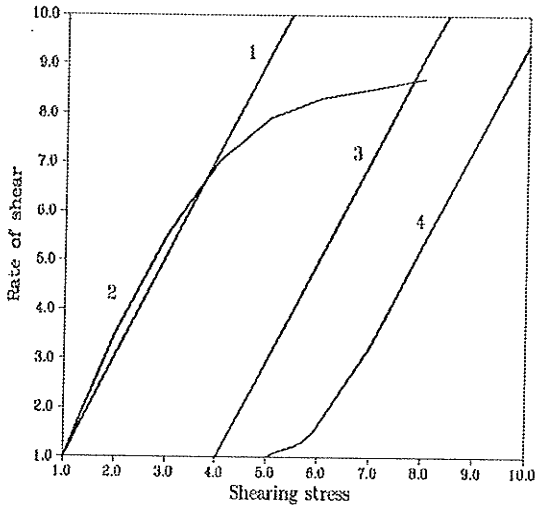

1 - Newtonian flow 2 - Dilatant flow
3 - Ideal plastic flow 4 - Bingham plastic flow

FIGURE 2.4 Relationships between shearing stress and rate of shear (Van Olphen, 1963)

In Figure 2.4, various shearing stresses (τ) versus rate of shear (D) relations are represented graphically. The rate of shear (D) is the velocity gradient perpendicular to the plane (Equation 2.14).

$$D = \frac{dV}{dx} \qquad [2.14]$$

where,

V = velocity of flow in the y-direction ($m\ s^{-1}$)

x = distance from a stationary surface (m)

The simplest relation is the linear relation illustrated by the straight line (1) which passes through the origin in the τ as a function of D graph, for which $\tau = \mu D$. Most

liquids obey this equation of flow. This type of flow is called Newtonian flow. The proportionality constant μ is called the coefficient of viscosity or, briefly, viscosity. It is independent of the shearing stress applied. Many systems display a more complicated flow behaviour. They are called, quite generally, non-Newtonian systems. Some common examples of non-Newtonian flow behaviour are illustrated by curves 2, 3 and 4 in Figure 2.4. At each point of these curves, an apparent viscosity can be defined. Alternatively, plastic viscosity or a differential viscosity at a certain rate of shear D can also be defined. The flow behaviour represented by curve 2 indicates an increase of the apparent and the differential viscosity with increasing rate of shear. In a system displaying a rheological behaviour represented by curve 3, no flow occurs until the shearing stress reaches a certain value τ_0. This value of the shearing stress at which the system begins to yield to the stress is called the yield stress. Beyond the yield stress value, the rate of shear is proportional to the shearing stress. The differential viscosity n is constant and the flow behaviour obeys the equation $\tau - \tau_0 = nD$. This type of flow is sometimes called ideal plastic flow. A slight departure from the flow behaviour represented by curve 3 is shown in curve 4. This type of flow which approximates ideal plastic flow is called Bingham plastic flow.

The viscosities of water in Na-montmorillonite systems at various water contents were calculated by Low (1976) by different equations using data from experiments conducted by different investigators for: (i) viscous flow of water at different temperatures, (ii) self diffusion of water, and (iii) neutron-scattering by water. The results showed that the viscosity of interlayer water is greater than that of bulk water and increases exponentially with decreasing water content (Low, 1976). The viscosity of a

solution of a single cationic species (for example, the interlayer solution) would be essentially a linear function of the concentration of that species (Low, 1979). There is complete unanimity among different investigators that water adsorbed on clay surfaces differs in structure and physical properties from bulk liquid water (Martin, 1962).

A steady-state nuclear magnetic resonance method was used (Pickett and Lemcoe, 1959) to investigate the shear strength of a clay water system. Plots of line width (a function of spin-spin relaxation time T_2, which is associated with internuclear coupling) as a function of moisture content, clearly showed that the viscosity of the water at the clay surface was greater than that of free water and that it decreased uniformly with increasing distance from the clay surface (Pickett and Lemcoe, 1959).

2.4 Movement due to gradients other than hydraulic gradients

An electric potential gradient causes electro-osmotic flow. The difference in the concentration of dissolved solids tends to cause liquid movement known as osmosis. The possible mechanisms causing intercepts in kaolinite were investigated using a constant-flow rate pump where the head difference across the sample for known flow rates was measured with a pressure transducer (Olsen, 1969). With this method, direct flow rate measurements and the associated errors from contaminant effect were avoided. The continuous relationship (typical data for the constant-flow-rate pump method) showed a finite flow rate intercept at zero hydraulic gradient. In contrast, the discontinuous relationship shows the existence of a threshold gradient (Figure 2.5).

Olsen (1985) showed that the continuous relationship could be displaced either upwards or downwards without changing its slope, by superimposing electrical or chemical gradients on a specimen during hydraulic permeability measurements

(Figure 2.6). Osmosis caused an intercept in the flow rate versus hydraulic gradient relationship that is consistent with the existing evidence for deviations from Darcy's law at low hydraulic gradients (Olsen, 1985).

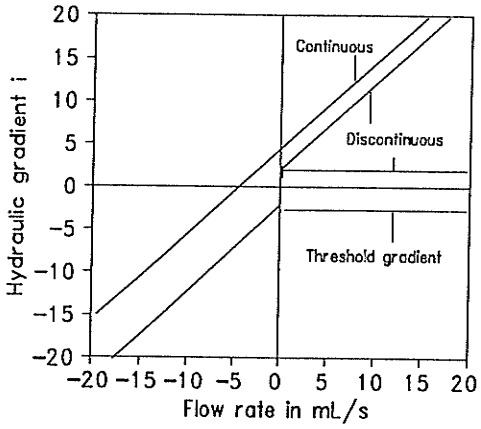

FIGURE 2.5 Continuous and discontinuous flow rate as a function of hydraulic gradient relationships for flow in opposite directions (Olsen, 1985)

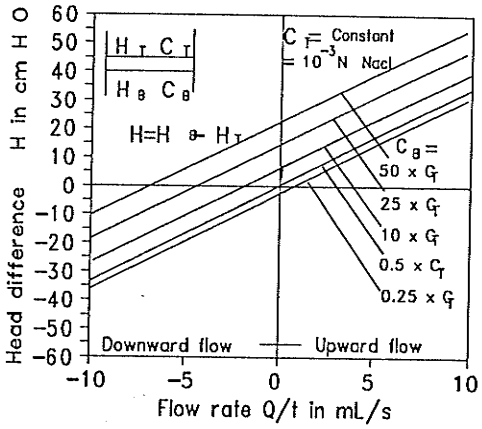

C_T,C_B - Electrolyte concentrations in the permeant at the top and bottom of the specimen, respectively

FIGURE 2.6 Measured head difference as a function of externally imposed flow rate (Olsen, 1985)

Generally, two transport mechanisms can be distinguished in clays:

(1) diffusion, for which the propelling force is the concentration gradient of the diffusing ions;

(2) advection, for which the propelling force is the hydraulic gradient

(Hasenpatt et al., 1989).

Even under significant hydraulic gradients, advection may be a minor process leaving molecular diffusion as the dominant transport process (Sri Ranjan and Gillham, 1991).

2.5 Suggested mechanisms

Two criteria must be met in a saturated clay sample for Darcy's law to be obeyed. First, liquid must exhibit Newtonian behaviour. Second, clay particles must be arranged in a skeleton sufficiently rigid to prevent seepage forces from modifying the architecture of the pore geometry (Olsen, 1966). A few mechanisms were proposed that provide possible ways in which these criteria can be violated:

1) **Existence of a quasi-crystalline structure in the water near clay surfaces.**

   A certain yield stress must be exceeded before the water structure can be deformed and, after that, the rigidity or viscosity of the water structure decreases with increasing shearing stress or hydraulic gradient (Low, 1961).

2) **Electroviscous component of resistance to liquid movement.**

   Electroviscous drag increases with increasing hydraulic gradient (Kemper, 1960).

3) **Seepage induced consolidation.**

   Seepage forces can consolidate a clay sample so that the pores are irreversibly diminished in size (Lutz and Kemper, 1959).

4) **Plugging and unplugging of flow channels.**

When finer particles move freely within the pores of the load-carrying skeleton of clay and coarse particles, seepage forces may cause these mobile particles to plug or unplug flow channels (Martin, 1962).

2.6 Properties of bentonite

Highly colloidal plastic clays, found originally near Fort Benton, Wyoming, U. S. A., were termed bentonite. Bentonite was defined as a rock composed essentially of a crystalline clay-like mineral formed by devitrification and the accompanying chemical alteration of a glassy igneous material, usually a tuff or volcanic ash (Ross and Shannon, 1926). These clays are composed largely of montmorillonite with small amounts of quartz, feldspar, volcanic glass, organic matter, gypsum and pyrite (Gillott, 1987).

The presence of a bentonite component in clays and soils may significantly affect properties of such materials and, hence, be of importance in agriculture, construction engineering and ceramics. Bentonites have a wide variety of uses in many different industries. Bentonite, particularly the sodium bentonite from Wyoming, is used extensively to impede the movement of water through earthen structures and retard or stop water movement through cracks and fissures in rock and concrete structures (Grim and Guven, 1978). Geological features and mineralogical studies of bentonites from locations all over the world are described in a review on properties of clays and its uses by Grim and Guven (1978).

3 Modelling Non-linear Saturated Flow through Sand and Bentonite Mixtures

3.1 Modified flow equation development

An equation is developed in this study to simulate the non-linear saturated flow through capillaries as a function of the imposed hydraulic conductivity based on an assumption about the viscosity as a function of distance from the surface of a particle in a porous matrix. Wyoming bentonite clay has been shown to have a viscosity different from the viscosity of free water out to distances from the clay surface in excess of 6 nm. The same should be true for other clay minerals with comparable atomic arrangements (Low, 1961). A viscosity ratio, viscosity of structured water to viscosity of free water, is used in this study to simulate the effect of forces of attraction near the clay surfaces inside the capillary tubes. This ratio is selected such that the modified flow line matches the data obtained from the samples.

Considering a circular pore with fluid of a single viscosity, the volumetric flow rate through a capillary is the integral of the velocity through the infinitesimal area $rd\theta dr$.

The equation of motion for steady laminar cylindrical flow is:

$$\frac{1}{r}\frac{d}{dr}(r\tau_{rz}) = -\frac{\Delta P}{\Delta Z} \qquad [3.1]$$

where,

τ_{rz} = z component of the shear stress associated with the momentum flux in the r-direction

r = radius (m)

P = pressure (Pa)

Z = length in the z-direction (m)

The modified flow equation for low-hydraulic-gradient flow through clays can be simulated with two viscosities, flow through structured water with a higher viscosity (μ^{II}) and flow through free water with the conventional values of viscosity (μ^{I}) (Figure 3.1).

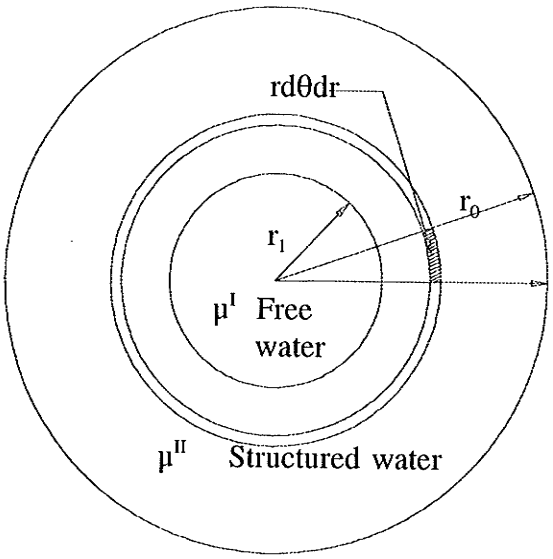

FIGURE 3.1 Cross section of a capillary tube

Integration of Equation 3.1 in the two regions results in the following relationships:

$$r\tau_{rz}^{I} = -\frac{1}{2}\frac{\Delta P}{\Delta Z}r^{2} + K_1^{I} \qquad [3.2]$$

$$r\tau_{rz}^{II} = -\frac{1}{2}\frac{\Delta P}{\Delta Z}r^{2} + K_1^{II} \qquad [3.3]$$

where,

τ^{I}_{rz} = z-component of the shear stress associated with the momentum flux in the r-direction in region I

τ^{II}_{rz} = z-component of the shear stress associated with the momentum flux in the r-direction in region II

K_1^{I} ,K_1^{II} = integration constants

Applying Newton's flow relation between rate of strain and stress,

$$\tau_{rz} = -\mu \frac{dv_z}{dr} \qquad [3.4]$$

where,

μ = viscosity (Pa s)

v_z = velocity in the z-direction (m s^{-1})

Substituting Equation 3.4 in Equations 3.2 and 3.3,

$$\frac{dv_z^{I}}{dr} = \frac{1}{2\mu^{I}} \frac{\Delta P}{\Delta Z} r + \frac{K_1^{I}}{\mu^{I} r} \qquad [3.5]$$

$$\frac{dv_z^{II}}{dr} = \frac{1}{2\mu^{II}} \frac{\Delta P}{\Delta Z} r + \frac{K_1^{II}}{\mu^{II} r} \qquad [3.6]$$

where,

μ^{I} = viscosity of free water (Pa s)

μ^{II} = viscosity of structured water (Pa s)

v_z^{I} = velocity of free water in the z-direction (m s^{-1})

v_z^{II} = velocity of structured water in the z-direction (m s^{-1})

Integrating Equations 3.5 and 3.6,

$$v_z{}^I = \frac{1}{4\mu^I}\frac{\Delta P}{\Delta Z} r^2 + \frac{K_1{}^I}{\mu^I}\ln r + K_2{}^I \qquad [3.7]$$

$$v_z{}^{II} = \frac{1}{4\mu^{II}}\frac{\Delta P}{\Delta Z} r^2 + \frac{K_1{}^{II}}{\mu^{II}}\ln r + K_2{}^{II} \qquad [3.8]$$

where,

$K_2{}^I$,$K_2{}^{II}$ = integration constants.

There are four integration constants in Equations 3.7 and 3.8. The four boundary conditions given below are used to obtain these constants.

1. $\frac{dv_z{}^I}{dr} = 0 \quad at \quad r = 0 \quad \therefore K_1^I = 0$

2. $\tau_{rz}^I = \tau_{rz}^{II} \quad at \quad r = r_1 \quad \therefore K_1^{II} = 0$

3. $v_z{}^I = v_z{}^{II} \quad at \quad r = r_1$

4. $v_z{}^{II} = 0 \quad at \quad r = r_0$

Therefore,

$$K_2^{II} = -\frac{1}{4\mu^{II}}\frac{\Delta P}{\Delta Z} r_0^2 \qquad [3.9]$$

and so

$$v_z^{II} = -\frac{1}{4\mu^{II}}\frac{\Delta P}{\Delta Z}(r_0^2 - r^2) \qquad [3.10]$$

Also,

$$K_2^I = -\frac{1}{4}\frac{\Delta P}{\Delta Z}\left(\frac{r_0^2}{\mu^{II}} + \frac{r_1^2}{\mu^I} - \frac{r_1^2}{\mu^{II}}\right) \qquad [3.11]$$

and so

$$v_z^I = -\frac{1}{4}\frac{\Delta P}{\Delta Z}\left(\frac{r_1^2}{\mu^I} - \frac{r^2}{\mu^I}\right) - \frac{1}{4}\frac{\Delta P}{\Delta Z}\left(\frac{r_0^2}{\mu^{II}} - \frac{r_1^2}{\mu^{II}}\right) \qquad [3.12]$$

where,

r_0 = radius of the capillary (m)

r_1 = radius of free flow (m)

Volumetric flow $\nabla^I + \nabla^{II} = \nabla$ [3.13]

where,

∇^I = volumetric flow of free water (region I) ($m^3\ s^{-1}$)

∇^{II} = volumetric flow through structured water (region II) ($m^3\ s^{-1}$)

∇ = Volumetric flow through the entire cross-section of the capillary tube ($m^3\ s^{-1}$)

$$\nabla^I = \int_0^{r_1} 2\pi r\, v_z^I\, dr = \frac{\pi}{8}\frac{\Delta P}{\Delta Z}\left(\frac{r_1^4}{\mu^I} + \frac{2r_0^2 r_1^2}{\mu^{II}} - \frac{2r_1^4}{\mu^{II}}\right) \qquad [3.14]$$

$$V^{II} = \int_{r_1}^{r_0} 2\pi r v_z^{II} dr = -\frac{\pi}{8}\frac{\Delta P}{\Delta Z}\left(\frac{r_0^4}{\mu^{II}} - \frac{2r_0^2 r_1^2}{\mu^{II}} + \frac{r_1^4}{\mu^{II}}\right) \quad [3.15]$$

From Equations 3.13, 3.14 and 3.15,

$$V = -\frac{\pi}{8}\frac{\Delta P}{\Delta Z}\left(\frac{r_0^4}{\mu^{II}} + \frac{r_1^4}{\mu^{I}} - \frac{r_1^4}{\mu^{II}}\right) \quad [3.16]$$

but,

$$V = q\ \pi r_0^2 \quad [3.17]$$

where,

q = flux (m s^{-1})

Also, in a horizontal tube, $\Delta P = \rho g \Delta h$ and so

$$\frac{\Delta P}{\Delta Z} = \rho g \frac{\Delta H}{\Delta Z} = \rho g i \quad [3.18]$$

where,

H = head of water (m)

ρ = density of water (kg m^{-3})

i = hydraulic gradient (m m^{-1})

Substituting Equations 3.17 and 3.18 in 3.16,

$$q = -\frac{\rho g}{8 r_0^2}\left(\frac{r_0^4}{\mu^{II}} + \frac{r_1^4}{\mu^{I}} - \frac{r_1^4}{\mu^{II}}\right) i \quad [3.19]$$

3.2 Modified flow model

Three parameters are used to characterize the flow behaviour based on Equation 3.19. Initially, under low hydraulic gradients, the water in the capillaries is structured and the viscosity is relatively higher due to forces of attraction. As the hydraulic gradient increases these forces become relatively less important and the flow becomes free initially at the centre. With further increases in hydraulic gradient, the cross-sectional area where free flow is occurring increases. This change continues until a certain hydraulic gradient is reached and the flow through the entire cross-sectional area can be regarded as free. At values of hydraulic gradient which exceed this hydraulic gradient the flow obeys Darcy's law as there is free flow in the entire cross-sectional area. The proposed model assumes a gradual increase in the effective cross-sectional area of free-water flow with increasing hydraulic gradient across the sample.

Three parameters, the hydraulic gradient at which flow through the entire cross-sectional area becomes free (transitional hydraulic gradient i_t), the equivalent diameter (an average capillary diameter representing the clay sample) and the ratio of viscosity of structured water to the viscosity of free water are used to simulate the non-linear flow pattern observed in the five-percent and ten-percent bentonite and sand samples.

3.2.1 Equivalent diameter $2r_0$

The equivalent diameter represents the average pore diameter of the sample. Equivalent diameter is selected individually for each sample such that the modified flow curve produced from Equation 3.19 best fits the data points in the higher hydraulic

gradient range. The effect of equivalent diameter on the simulated flux as a function of the hydraulic gradient relationship is shown in Figure 3.2. The curve representing flux as a function of the imposed hydraulic gradient can be shifted upwards or downwards by selecting a higher or lower equivalent diameter. On a log-log plot of flux versus the hydraulic gradient, the hydraulic conductivity in the higher hydraulic gradient range is given by the flux value at the intersecting point of the 1:1 slope line representing the data points in the higher range and the vertical line at hydraulic gradient of one.

3.2.2 Transitional hydraulic gradient i_t

The hydraulic gradient at which the flow through the entire cross sectional area becomes free is termed the transitional hydraulic gradient. The radius of free flow r_1 is considered to increase linearly with the increase in the imposed hydraulic gradient.

From Equation 2.5 and 3.19,

$$K = -\frac{\rho g}{8 r_0^2}\left(\frac{r_0^4}{\mu^{II}} + \frac{r_1^4}{\mu^{I}} - \frac{r_1^4}{\mu^{II}}\right) \qquad [3.20]$$

The ratio of r_1 / r_0 goes linearly from zero to one as the imposed hydraulic gradient goes from zero to the transitional hydraulic gradient.

$$r_1 = \left(r_0 \quad \frac{i}{i_t}\right) \qquad 0 < i \le i_t \qquad [3.21]$$

Substituting Equation 3.21 in Equation 3.20,

$$K = \frac{\rho g}{8 r_0^2}\left(\frac{r_0^4}{\mu^{II}} + \frac{\left(r_0 \frac{i}{i_t}\right)^4}{\mu^{I}} - \frac{\left(r_0 \frac{i}{i_t}\right)^4}{\mu^{II}}\right) \qquad 0 < i \le i_t \qquad [3.22]$$

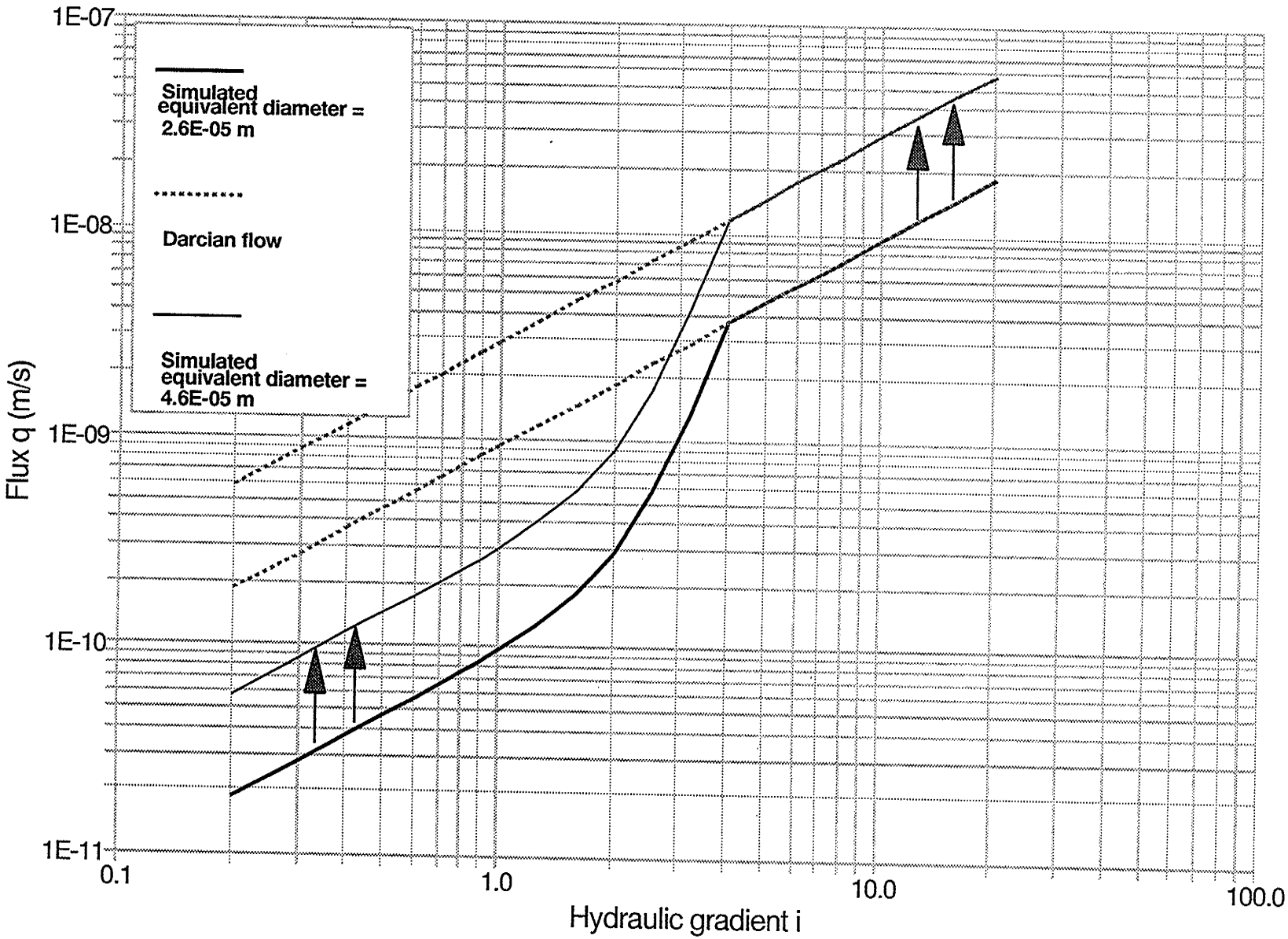

FIGURE 3.2 Influence of equivalent diameter on the simulated flux

$$K = \frac{\rho g\ r_0^2}{8}\left(\frac{\left(1 - \left(\frac{i}{i_t}\right)^4\right)}{\mu^{II}} + \frac{\left(\frac{i}{i_t}\right)^4}{\mu^{I}}\right) \qquad 0 < i \leq i_t \qquad [3.23]$$

$$K = \frac{\rho g\ r_0^2}{8\ \mu^{I}} \qquad i_t < i \qquad [3.24]$$

Equation 3.23 shows the dependence of hydraulic conductivity on the imposed hydraulic gradient below the transitional hydraulic gradient i_t. The value of transitional hydraulic gradient is selected such that the non-linear flow model best fits the sample data in the hydraulic gradient range below the transitional hydraulic gradient. The effect of the transitional hydraulic gradient on the simulated flux as a function of the hydraulic gradient relationship is shown in Figure 3.3. This figure shows the effect of the transitional hydraulic gradient on the point at which the non-linear flow becomes Darcian linear flow.

3.2.3 Viscosity ratio of structured water to free water μ^{II} / μ^{I}

The effect of imposed hydraulic gradient on the forces of attraction near the clay surface can be simulated by choosing two different viscosities for the structured and free water in the capillaries. When the attractive forces near the clay surfaces are relatively more important, the state of water is represented by structured water with a higher viscosity. These forces of attraction become less important as the as the distance from the clay surface increases and this state is represented by the viscosity of free water. The value of the higher viscosity is selected such that the modified flow line below the

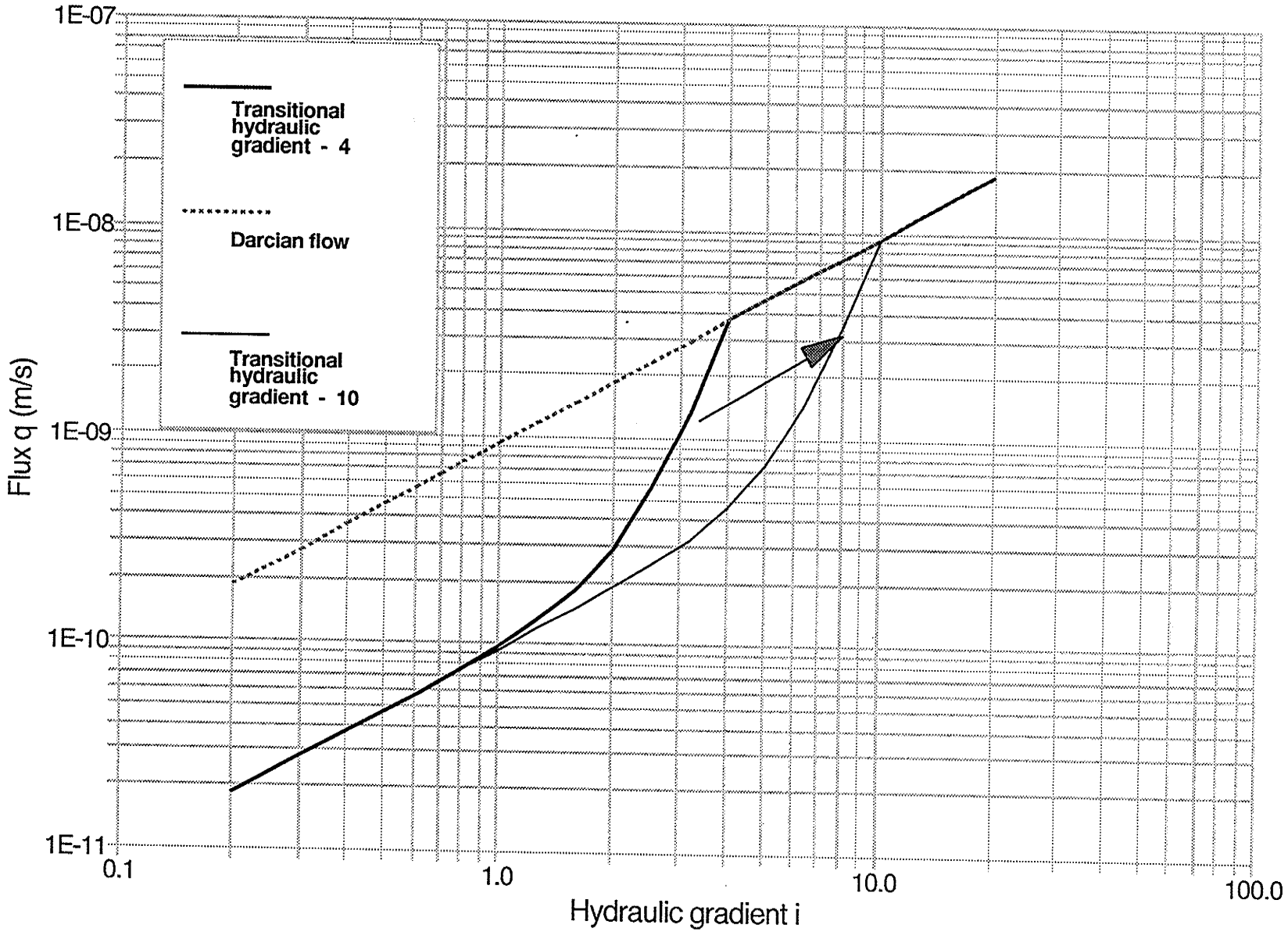

FIGURE 3.3 Influence of transitional hydraulic gradient on the simulated flux

transitional hydraulic gradient matches the data of different samples. This higher viscosity value is given as a ratio with reference to the viscosity of free water. The change in simulated flux due to change in the ratio of viscosity of structured water to free water is shown in Figure 3.4. In Figure 3.2, the whole curve can be shifted upwards by increasing the equivalent diameter but in Figure 3.4 only the low-hydraulic-gradient flow section can be shifted vertically by selecting a higher viscosity ratio.

The flux as a function of hydraulic gradient relationships for the ten-percent bentonite and sand mixtures can be simulated by both a spreadsheet and a Fortran 77 program (Appendix I). Data from different clay types have to be obtained to determine the model parameters for each clay type and bulk density.

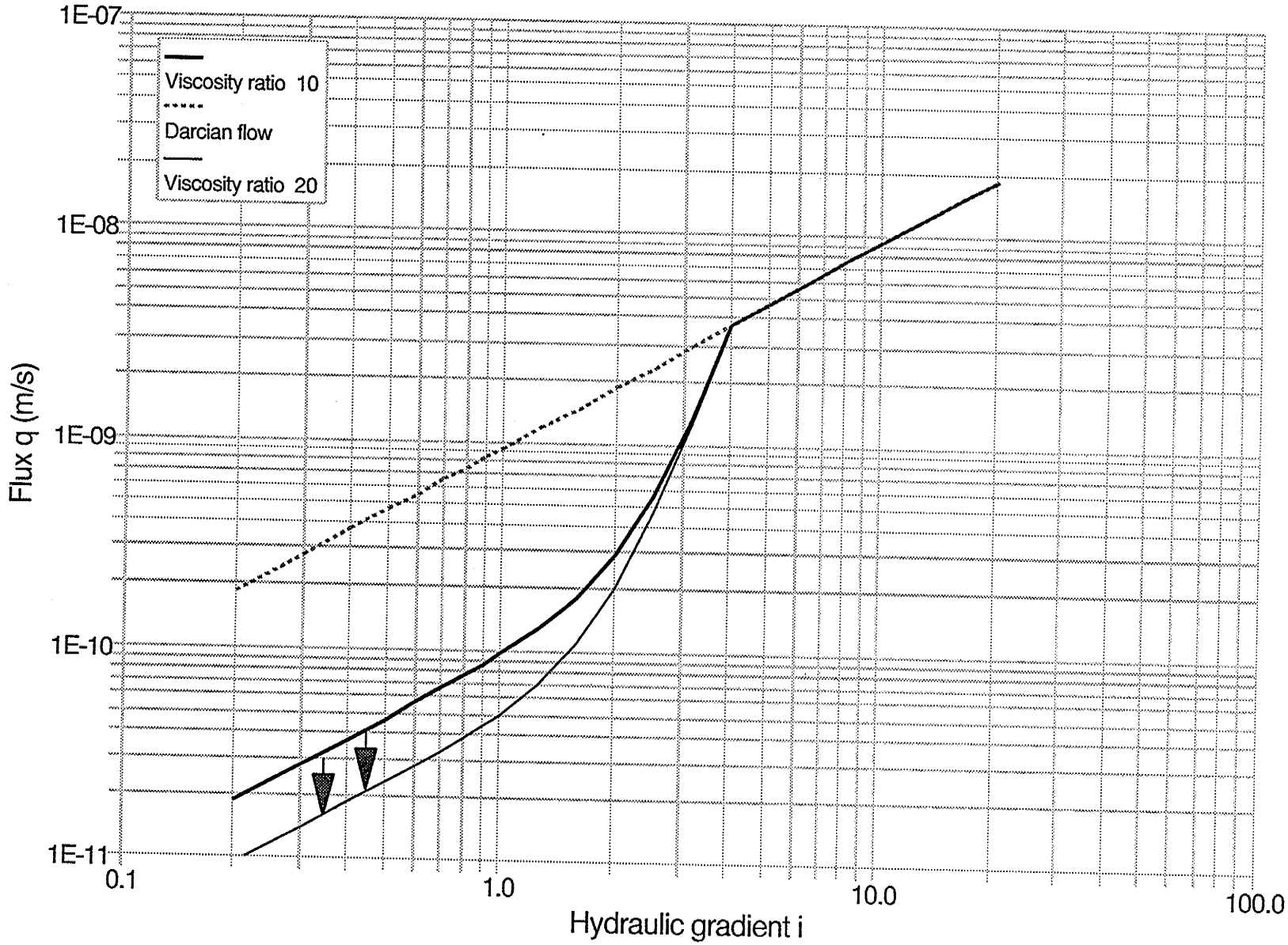

FIGURE 3.4 Influence of viscosity ratio on the simulated flux

3.3 Estimation of equivalent diameter using the Kozeny-Carman equation

The equivalent diameter can also be estimated using the Kozeny-Carman equation:

$$k = \frac{\phi^3}{K_s \; T \; s^2} \qquad [3.25]$$

where,

k = intrinsic permeability (m^2)

K_s = dimensionless shape factor

T = tortuosity

ϕ = porosity ($m^3 \; m^{-3}$)

s = specific surface ($m^2 \; m^{-3}$)

$$K = \frac{k \; \rho \; g}{\mu} \qquad [3.26]$$

Hydraulic conductivity depends on both the fluid and the soil characteristics:

where,

K = hydraulic conductivity ($m \; s^{-1}$)

μ = fluid viscosity (Pa s)

ρ = fluid density ($kg \; m^{-3}$)

g = gravitational acceleration ($m \; s^2$)

An average pore size or an equivalent diameter can be defined as:

$$\bar{d} = \frac{\phi}{s} \qquad [3.27]$$

where,

$\bar{d}$ = equivalent diameter (m)

From Equations 3.25 , 3.26 and 3.27,

$$\bar{d} = \left(\frac{K K_s T \mu}{\phi \rho g} \right)^{\frac{1}{2}} \qquad [3.28]$$

The measured hydraulic conductivity values and the known or estimated values of the other parameters can be substituted in Equation 3.28 to estimate the equivalent diameter of the samples.

4 Methodology

4.1 Sample holder

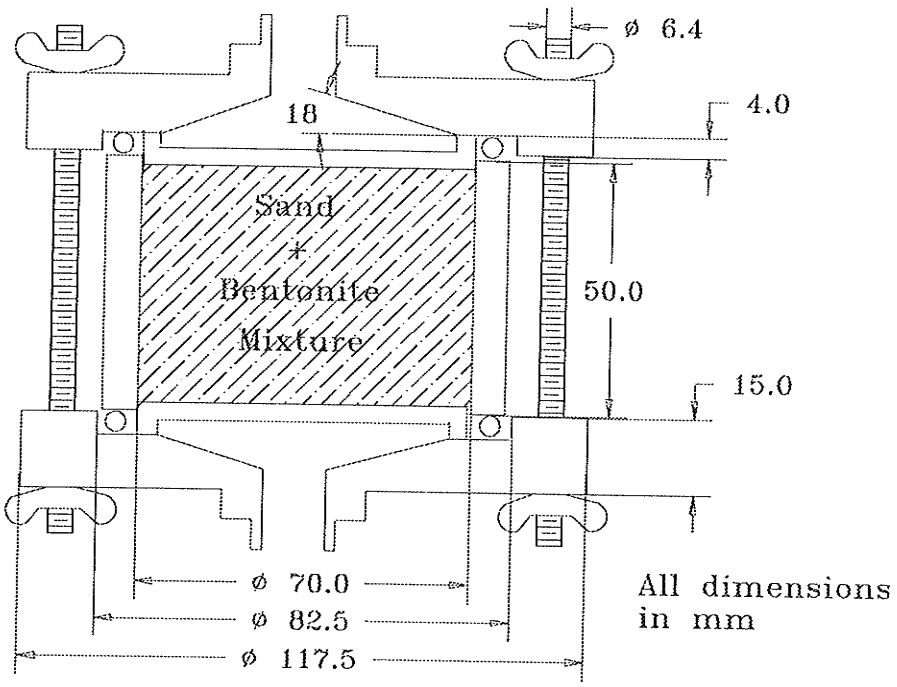

FIGURE 4.1 Sample holder

Precision-machined cylindrical sample holders (Figure 4.1) designed to allow one-dimensional flow were used to pack the ten-percent Na-Bentonite and fine sand (Selkirk silica sand - 150-200 μ m-diameter) mixtures. The height of all cylinders was 50 mm. End plates and cylinders were cut and machined out of plexiglass plates and cylindrical tubes, respectively. Three 6.4-mm-outside-diameter stainless steel rods, butterfly nuts and "O" rings were used to keep the cylinder with the endplates airtight. The inner side of the end plates was machined and polished to produce a smooth 18° concave surface to facilitate saturation of the sample.

Inflow and outflow lines were connected to the holder with teflon fittings. Thick-wall 6.4-mm-outside-diameter and 3.2-mm-inside-diameter teflon tubing was used to connect the sample holder with the flow meter.

4.2 Liquid bubble flow meter

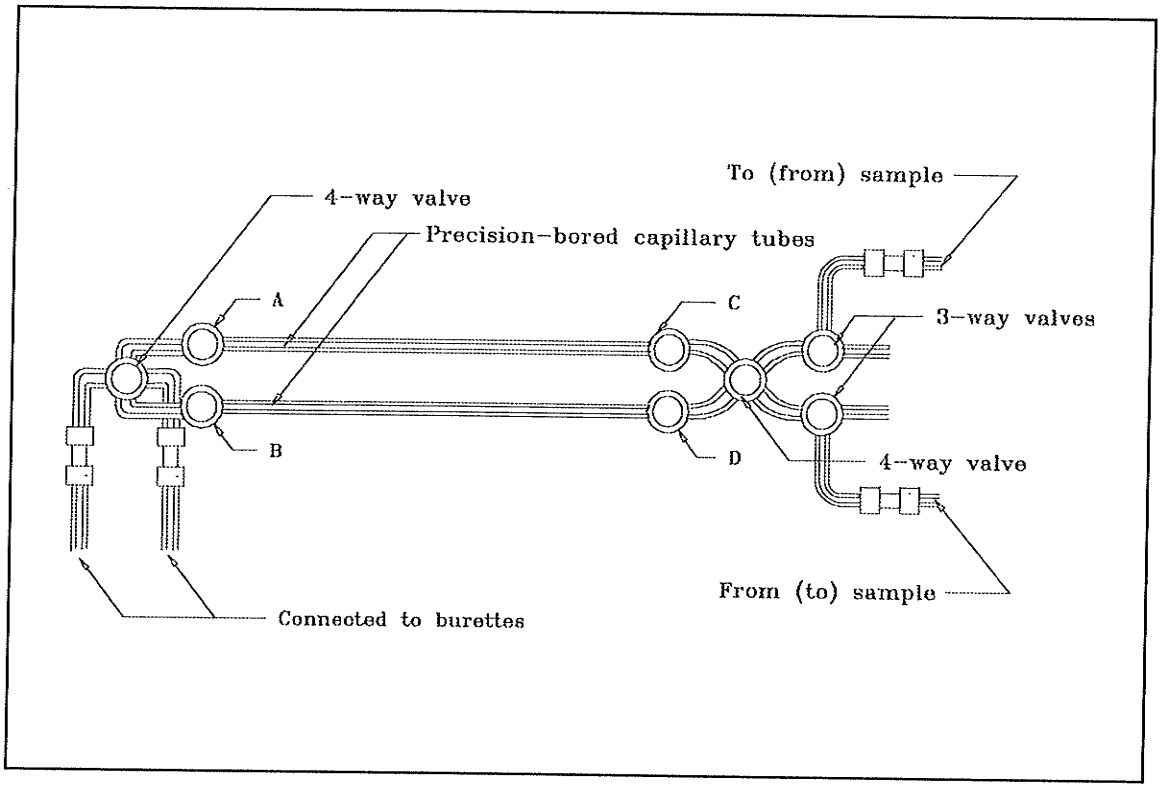

FIGURE 4.2 Improved liquid bubble flow meter

The main objective of this thesis project was to measure the hydraulic flow through Na-bentonite and sand mixtures under low hydraulic gradients using an improved flow meter. The liquid bubble flow meter (Figure 4.2) was used to measure both inflow and outflow through the sample.

Mechanical leakage in the external fittings is an important source of error (Tavenas et al., 1983). A liquid bubble flow meter was built with precision

0.8-mm-inside-diameter capillary tubes and greaseless-type teflon fittings to minimize leakage. The greaseless type was chosen to avoid contamination of the capillary tubes. The ends of the tubes were connected to four-way valves so that the direction of flow could be reversed. Capillary tubes were cleaned with both acid and a commercial cleaner to minimize the contamination effect on the inner surface of the tube.

Conventional flow meters of the past used an air bubble in capillary tubes or air water menisci that were affected by contamination of the inner surface of the capillary tubes (Olsen, 1965). To overcome the resistance to flow by air bubbles and to minimize the instrument threshold, perchloro-ethylene with Sudan IV (a red coloured dye) was used as the bubble liquid. Perchloro-ethylene is highly soluble in alcohol and ether but it is insoluble in water. As a common solvent used in dry cleaning, it also has a self-cleaning ability.

Advancing menisci in both inflow and outflow capillary tubes were observed through microscopes mounted on electronic calipers (Figure 4.3). Each millimetre of the 2.4-mm micro-scale in the eyepiece of the microscope was divided into 50 small divisions. This increased the precision of the instrument. The microscope-electronic caliper assembly was mounted on a metal bar that was fixed parallel to the capillary tubes (Figure 4.4).

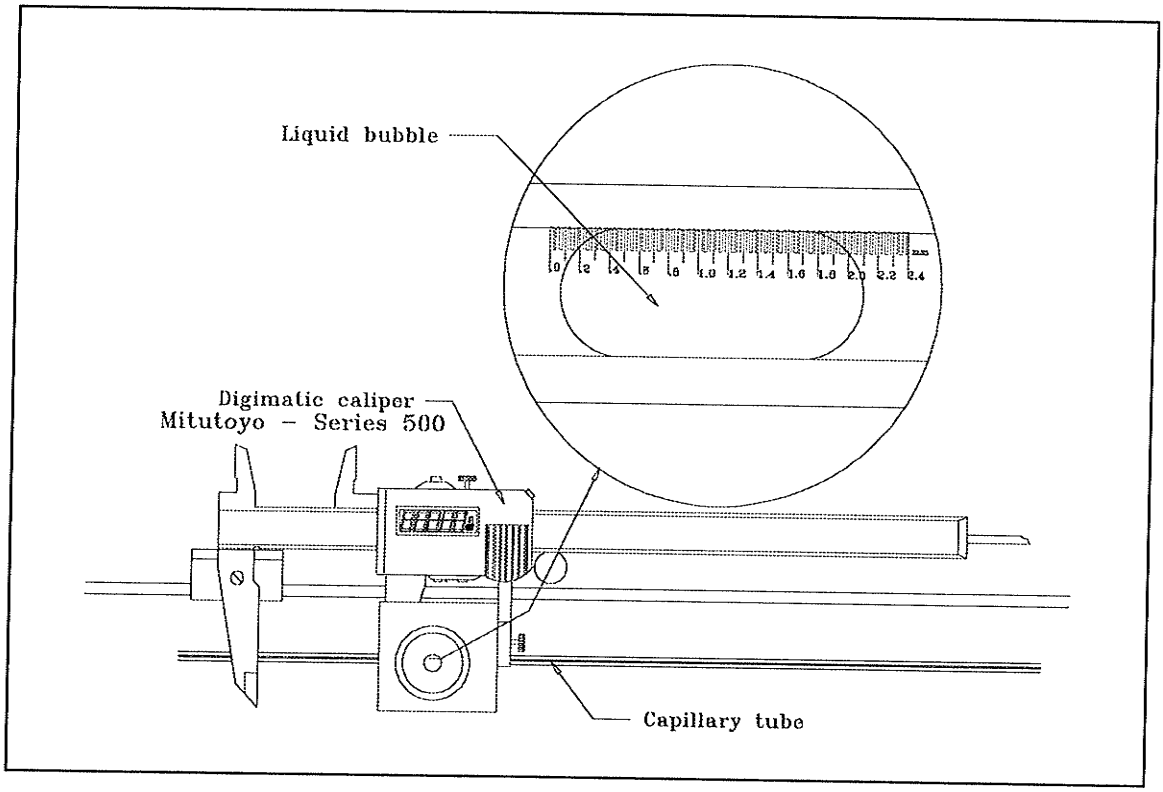

FIGURE 4.3 Mini-microscope mounted on the electronic caliper

The sample holder was enclosed in a temperature-controlled insulated chamber capable of maintaining ±0.1 °C from a predetermined temperature. The chamber temperature was recorded by a computer program using a calibrated thermistor (Fenwal thermistor - 192-103LET-AO1, 10,000 ohms @25°C ± 0.2%) . A sample temperature profile is shown in Figure 4.5. The chamber temperature had a logarithmic relationship with thermistor resistance (Figure 4.6).

The effective stress of the sample was kept relatively constant by lowering the outflow side and raising the inflow side by equal amounts. This was achieved by a left-hand and a right-hand screw-thread arrangement connecting the inflow and outflow

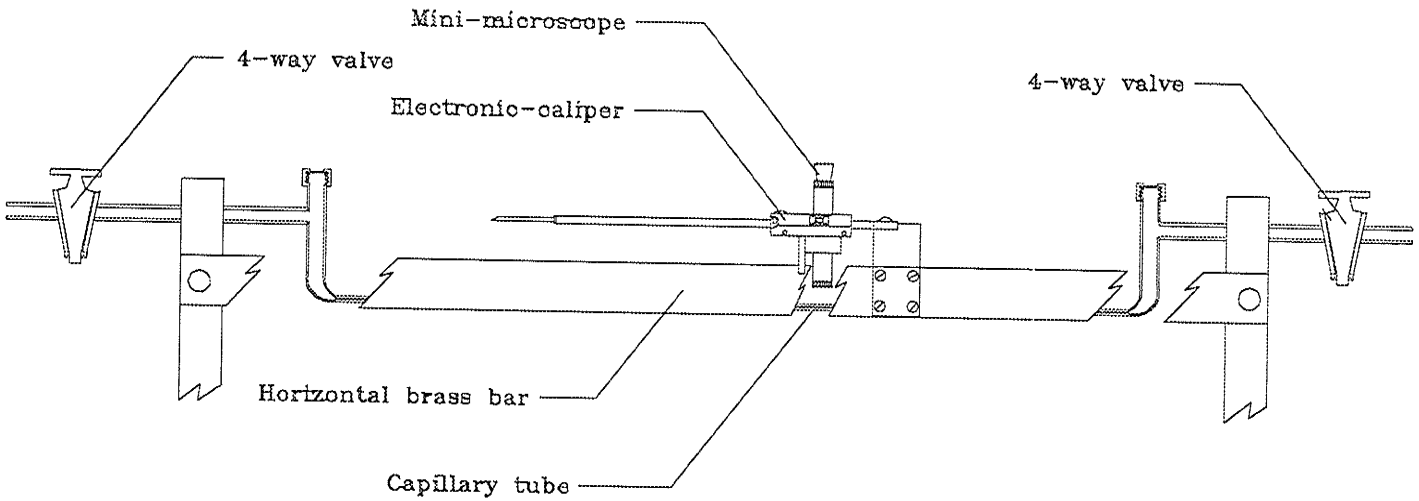

FIGURE 4.4 Side view of mini-microscope mounted on the electronic caliper

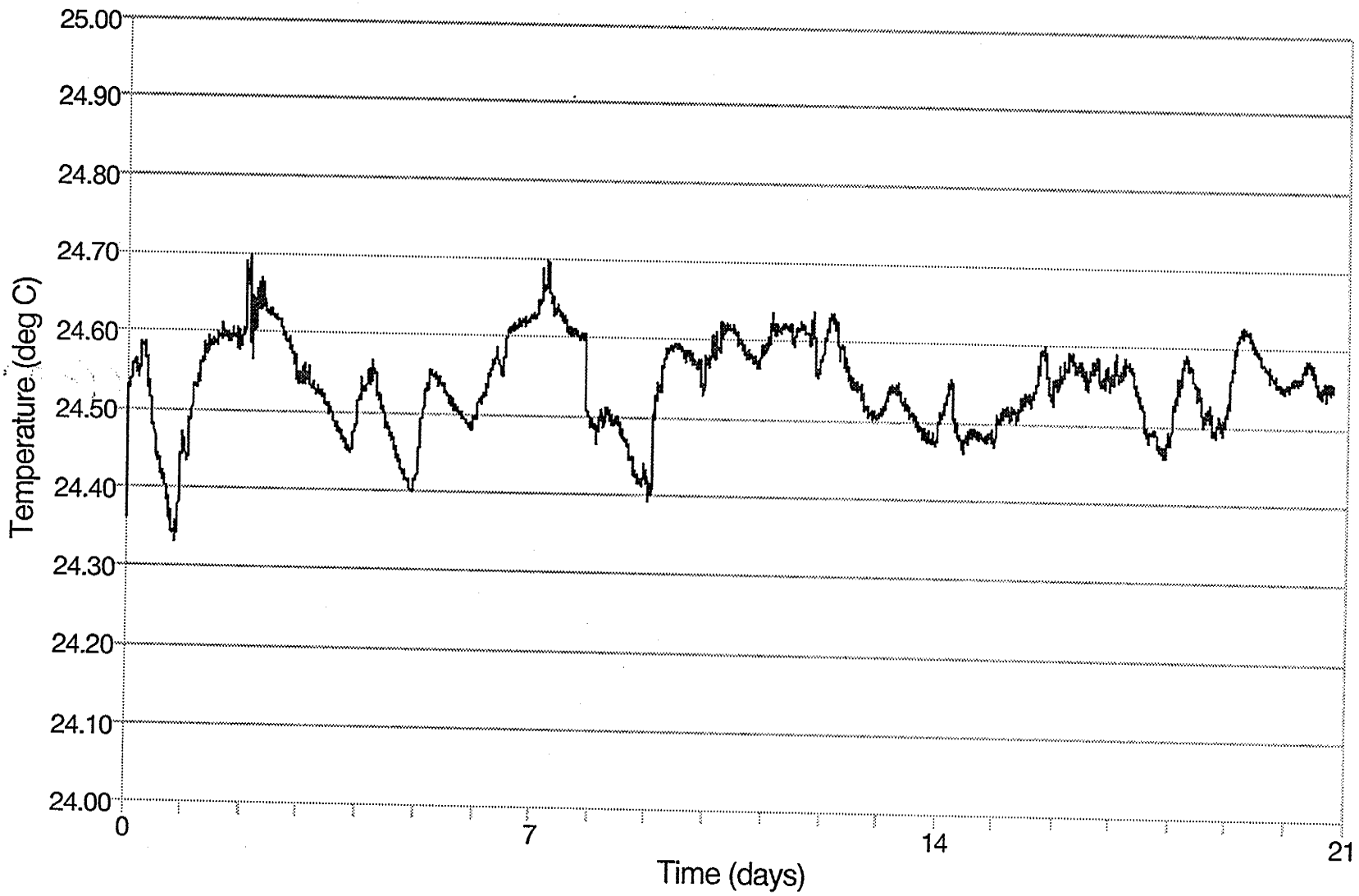

FIGURE 4.5 Chamber temperature recorded using a thermistor

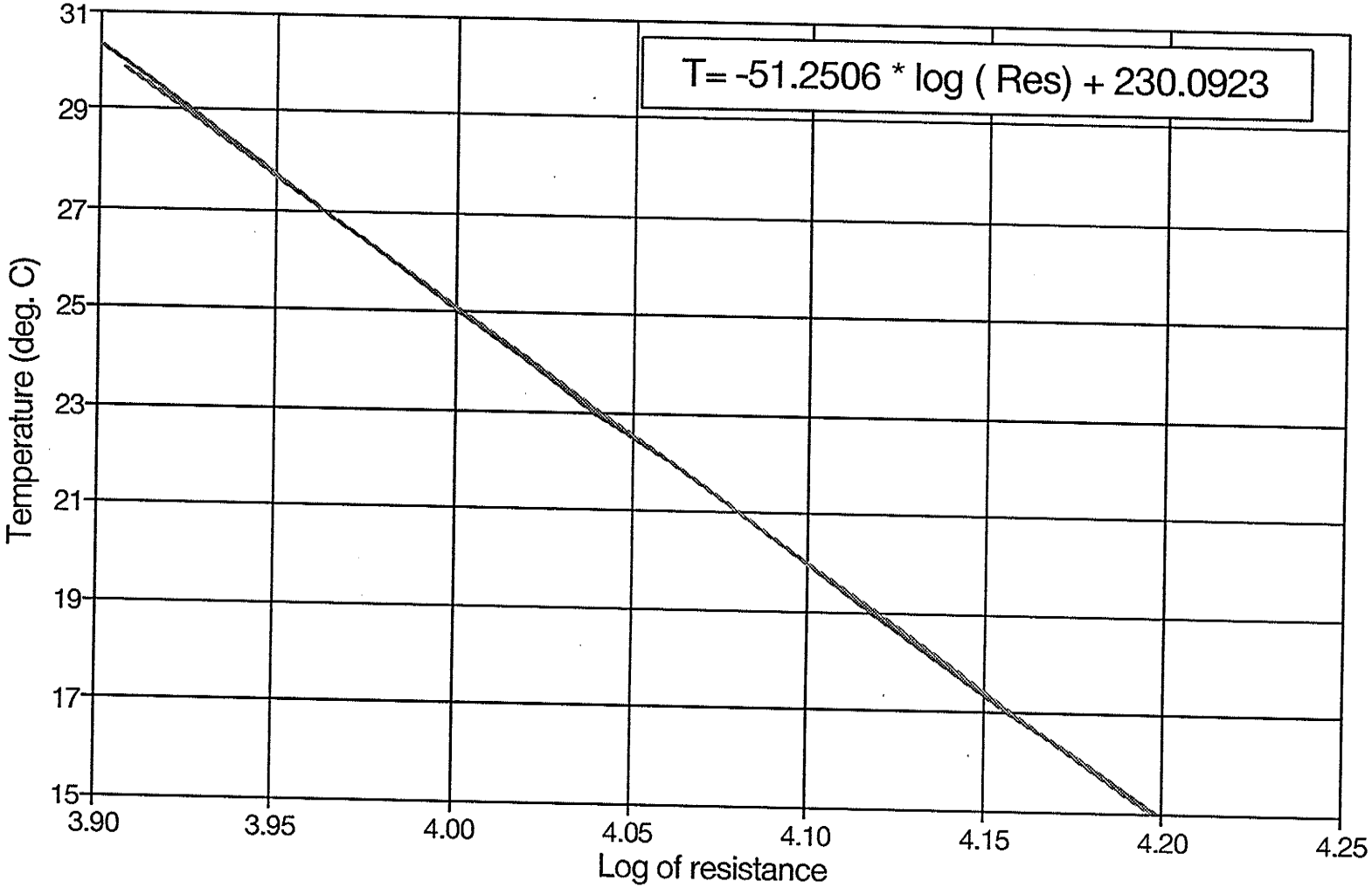

FIGURE 4.6 Semi-logarithmic plot of temperature versus thermistor resistance

frames, respectively. When the sample had stabilized in the experimental setup, inflow and outflow measurements were taken for small increments of head differences while maintaining a relatively constant effective stress on the sample.

4.3 Sample preparation

Two sets of ten-percent and five-percent Na-bentonite (by weight) and sand (Selkirk silica sand - 150-200-μm-diameter) mixtures were prepared and packed in 70-mm-diameter cylindrical sample holders. The dry bulk density of the samples was 1.44 Mg m^{-3}. Since non-uniform distribution of bentonite could result in increased permeabilities at locations of low bentonite content, care was taken to pack uniformly (Wang and Huang, 1984). A measured amount of dry bentonite was first thoroughly mixed with sand several times to achieve uniformity across the samples. The dry mixture was packed inside the cylinder resting on the bottom endplate.

All six samples were held vertically in a wooden frame and CO_2 gas was passed through the samples for nine days to displace the air in the pore space. De-ionized de-aired water was allowed through the bottom of the samples and the flow was controlled to permit a slow-moving wetting front in each of the samples. These steps reduced the chances of trapping air bubbles during the saturation process.

The first sample was removed after two weeks and kept inside the temperature-controlled chamber to equilibrate for two days before the measurements on the sample commenced. One sample at a time was kept inside the chamber. Measurements on each of these samples were completed within six weeks.

4.4 Measurement of flux through the samples

The inflow rate and outflow rate were measured separately. Repetitive measurements of flux were taken for each set level of hydraulic gradient in both inflow and outflow capillaries. The advancing meniscus of the bubble was aligned with a reference point in the graticule in the microscope and the caliper was zeroed. As the bubble moved, the microscope was also moved along and aligned with the new position of the bubble. The electronic caliper reading gave the distance between the initial point and the final point. The elapsed time was recorded using a stop-watch. The flux through the sample holder was calculated by multiplying the flux through the capillary tube by the ratio of cross-sectional-area of capillary tube to the cross-sectional-area of the sample holder.

The measured outflow rate was different from the inflow rate for the same imposed hydraulic gradient. The difference between the two flow rates was used as a guide in determining equilibrium. When the difference between the outflow rate and the inflow rate was within two to three times the outflow rate the measurements were recorded. Although the inflow rate and outflow rate measured at the same time fluctuated, the difference between the overall average of the inflow rates and the overall average of outflow rates for a set level of gradient was very small. Therefore only the outflow values were used in the analysis. The hydraulic conductivity values below the transitional gradient were obtained from the log-log plot of flux versus the imposed hydraulic gradient (Figure 4.7).

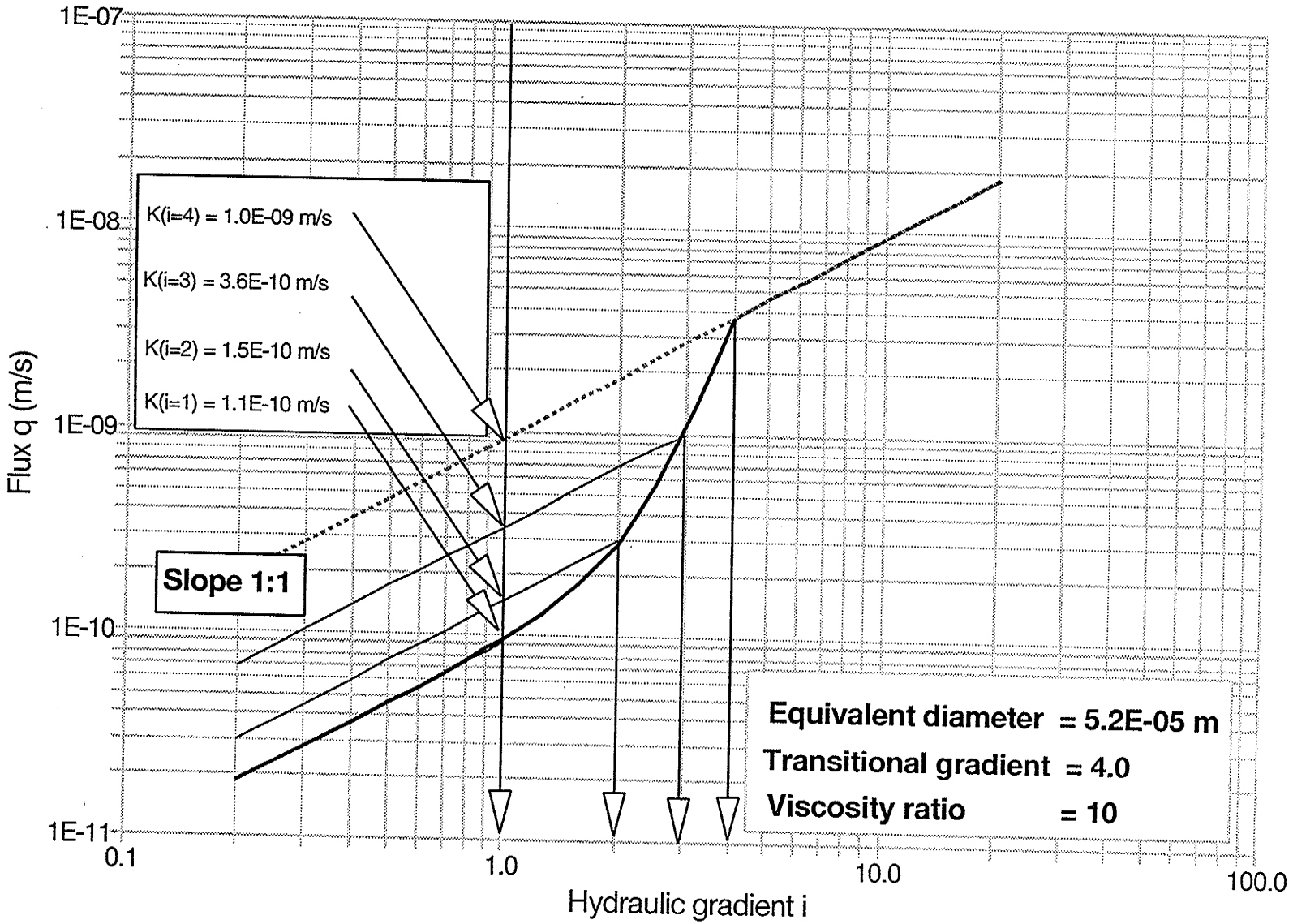

Figure 4.7 Hydraulic conductivity values below transitional hydraulic gradient

5 Results and Discussion

As mentioned in Chapter 4, the inflow rate and outflow rate were measured separately. In each of the samples, repetitive measurements were taken for each of the set levels of hydraulic gradient. The measured outflow rate was different from the inflow rate for the same imposed hydraulic gradient. The difference between the two flow rates was used as a guide in determining equilibrium. It was postulated that the lower the difference the higher the degree of saturation of the sample had become. Only the outflow values were analyzed. If Darcy's linear flow equation were used to model the flow, the flux as a function of hydraulic gradient should be a linear plot going through the origin.

5.1 Non-linearity in five-percent and ten-percent bentonite and sand samples

Tthe five-percent bentonite and sand samples 5P1, 5P2 and 5P3 (Figures 5.1 to 5.3) and the ten-percent bentonite and sand samples 10P4, 10P5 and 10P6 (Figures 5.4, to 5.6) show that the data deviate from the Darcian proportional line below a hydraulic gradient of four. Horizontal markers in Figures 5.1 to 5.6 represent ± standard error (S E) from the mean.

Experimental evidence on five-percent bentonite and sand mixtures indicates that, under low hydraulic gradients, the hydraulic conductivity could vary by an order of magnitude from the value which would be obtained under high hydraulic gradients (Sri Ranjan and Karthigesu, 1992). The average of inflow and outflow of the five-percent bentonite and sand samples shows that the hydraulic conductivity value below a hydraulic gradient of one was about three times less than the value obtained for higher hydraulic

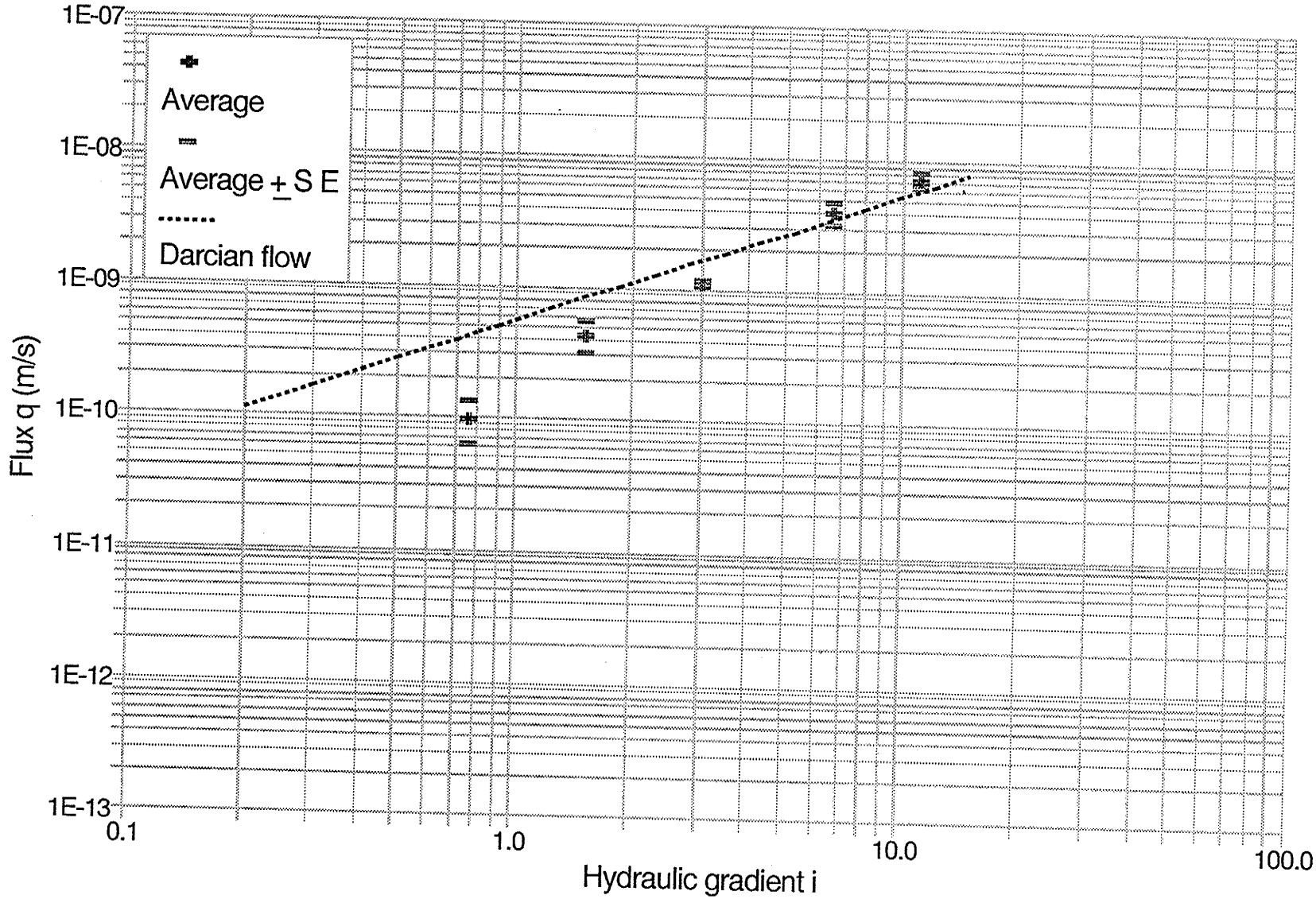

FIGURE 5.1 Flux versus hydraulic gradient - 5P1

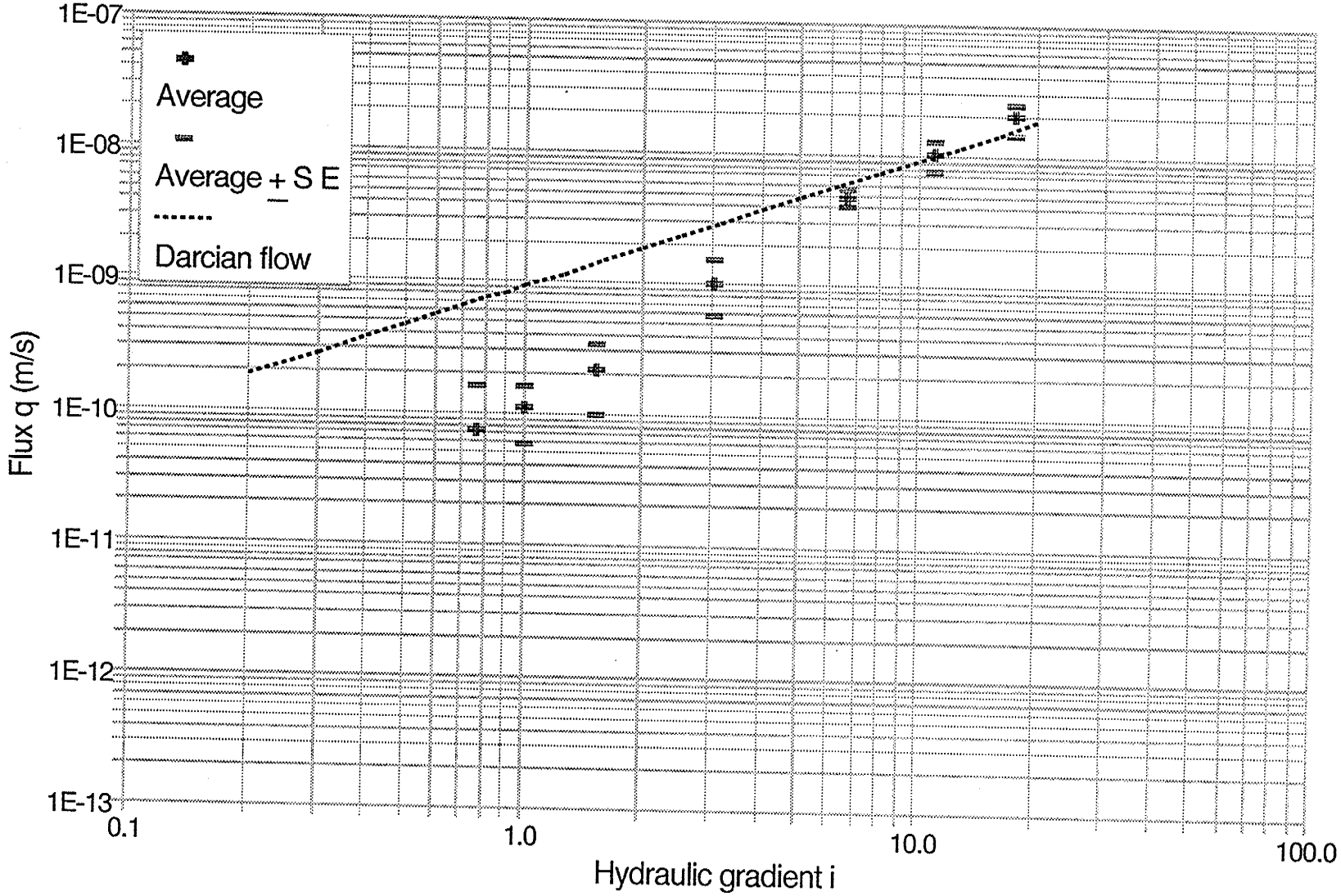

FIGURE 5.2 Flux versus hydraulic gradient - 5P2

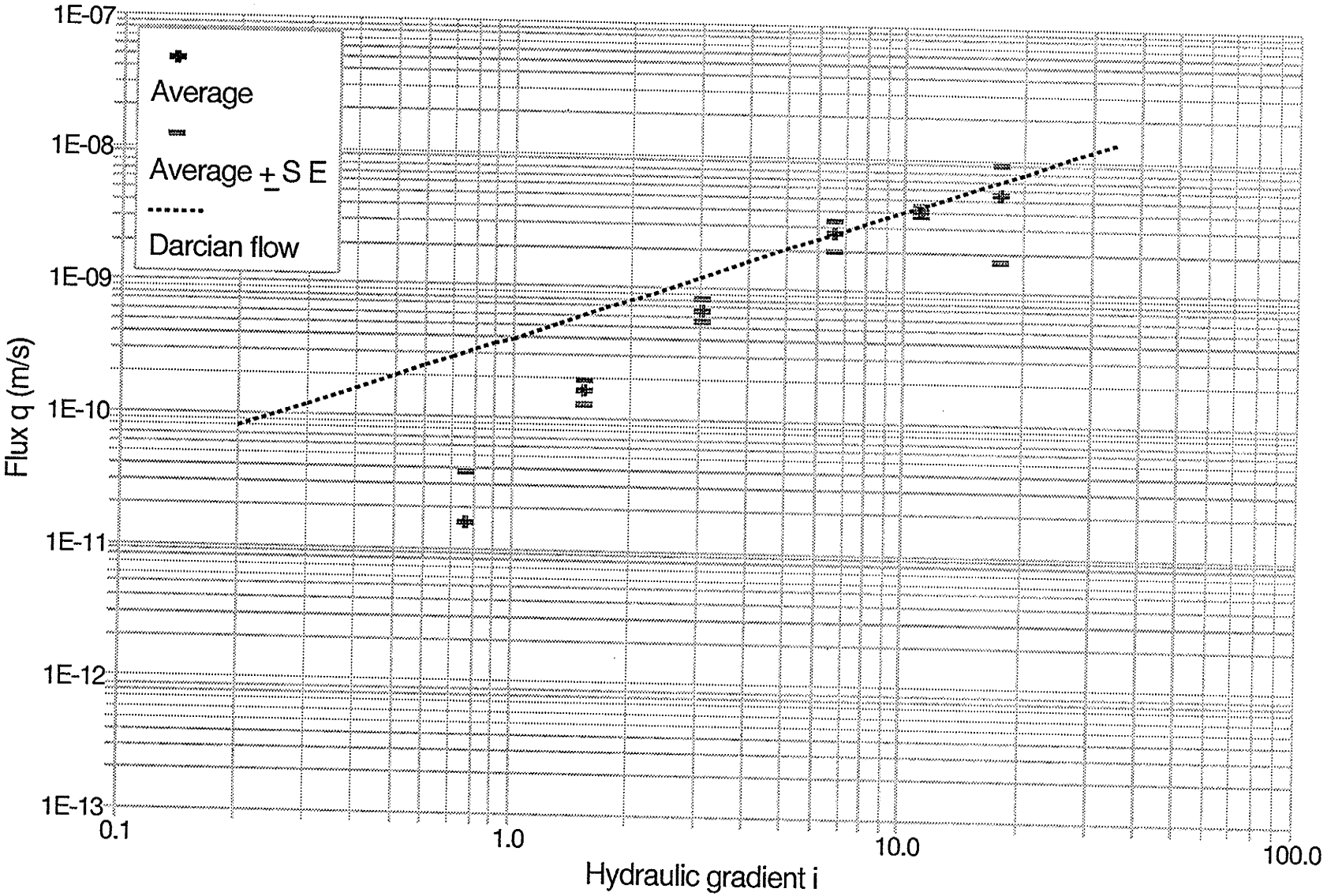

FIGURE 5.3 Flux versus hydraulic gradient - 5P3

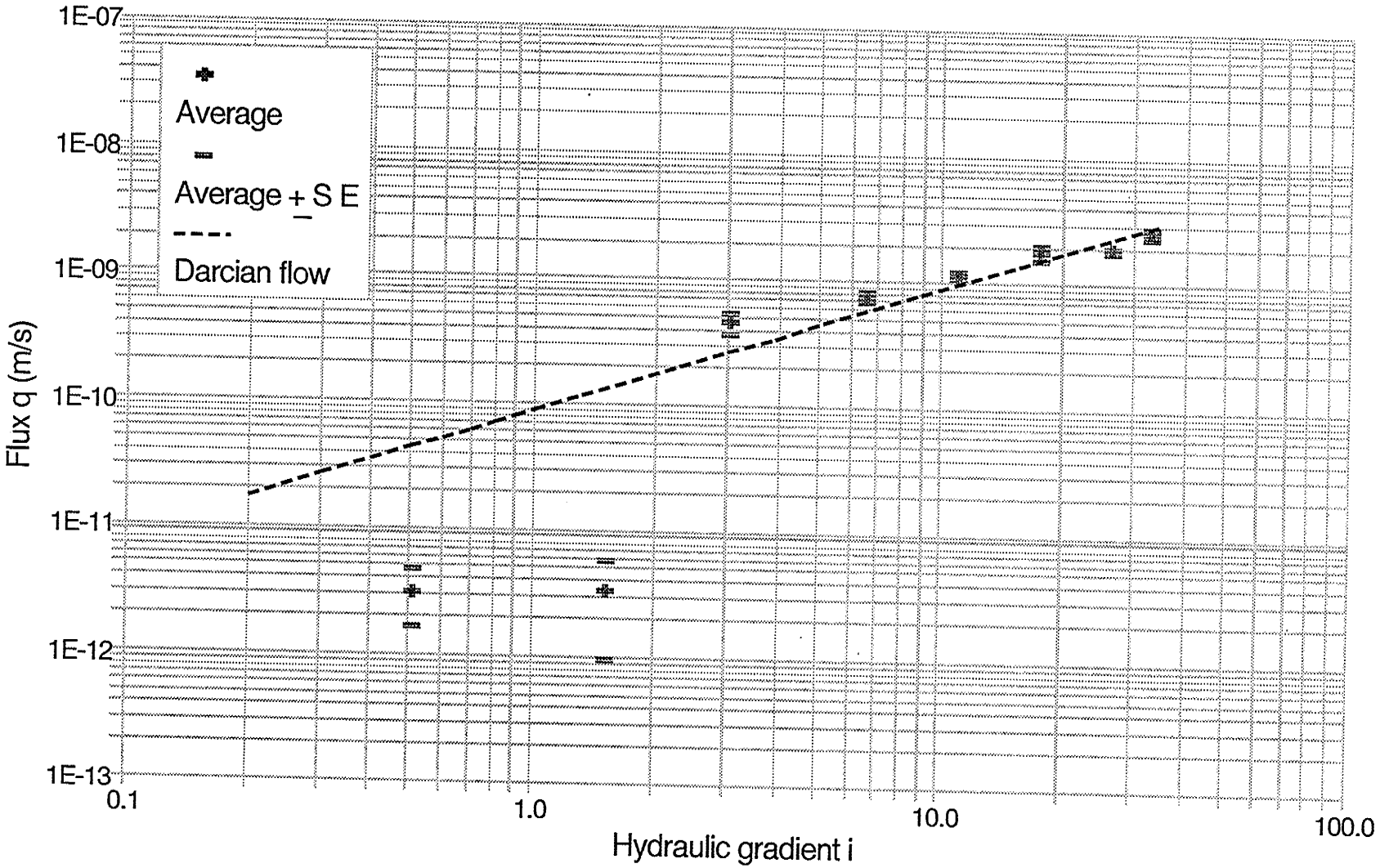

FIGURE 5.4 Flux versus hydraulic gradient - 10P4

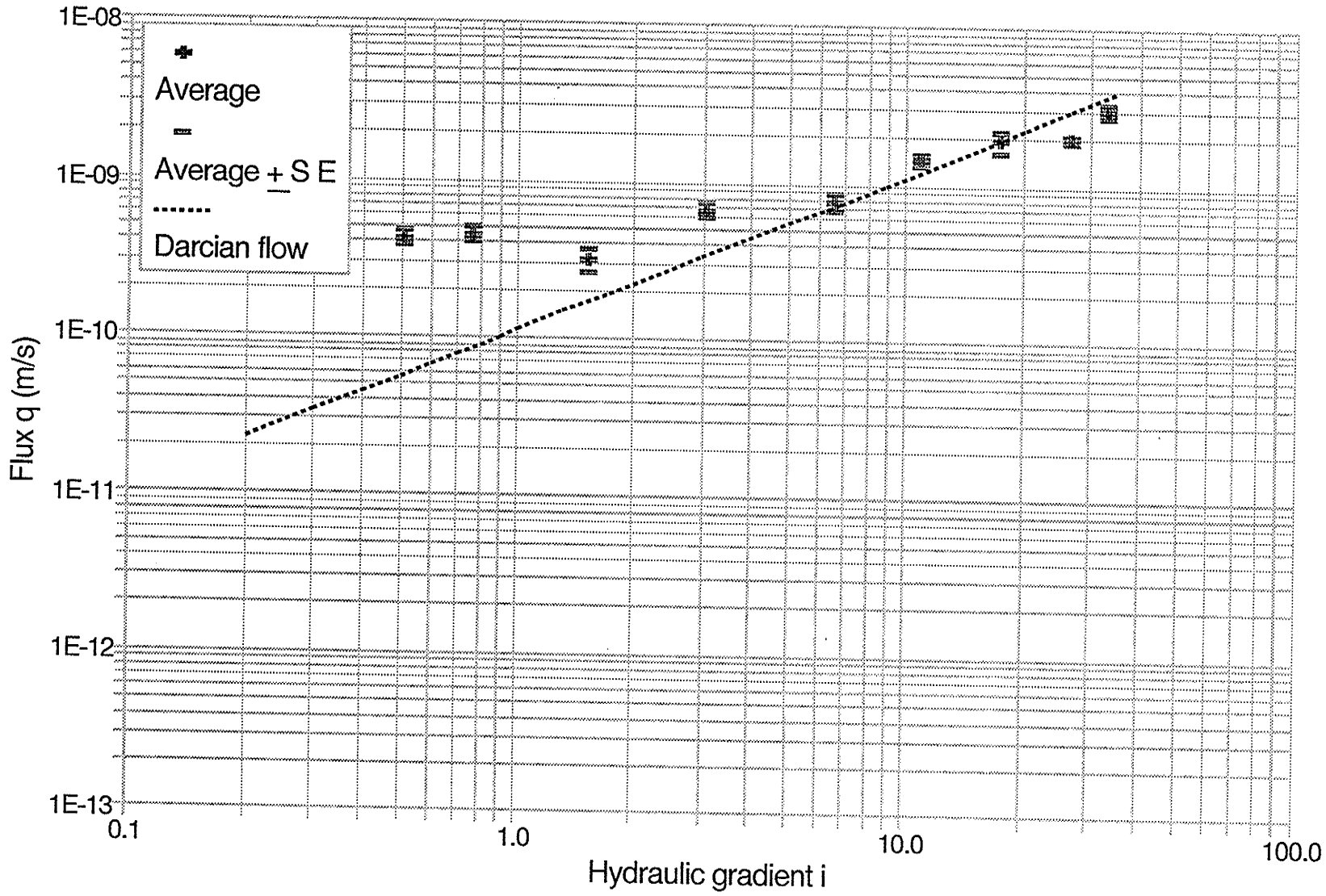

FIGURE 5.5 Flux versus hydraulic gradient - 10P5

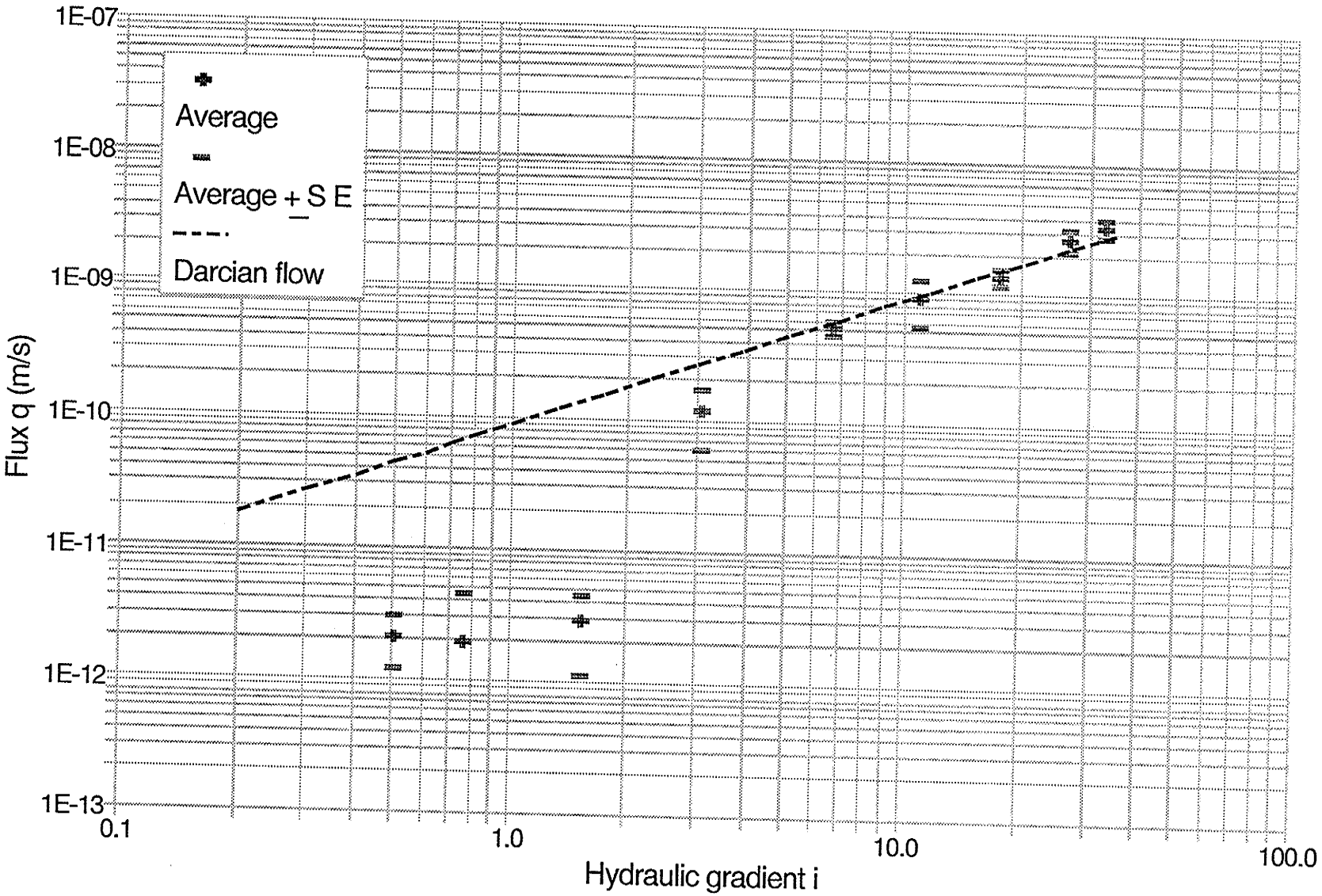

FIGURE 5.6 Flux versus hydraulic gradient - 10P6

gradients. Except for 10P5, this change was more pronounced in the ten-percent bentonite and sand samples (Karthigesu and Sri Ranjan, 1992). The higher flow rate observed in the ten-percent bentonite and sand sample 10P5 may have been be due to leakage in the fittings.

5.2 Parametric values used in the proposed model simulation

The five-percent bentonite and sand samples and the ten-percent bentonite and sand samples (except for 10P5) show that the hydraulic conductivity is dependent on the imposed hydraulic gradient below a hydraulic gradient of four (Figures 5.7 to 5.11). Hydraulic conductivity increases with the increase in the imposed hydraulic gradient below the transitional hydraulic gradient (Figures 5.7 to 5.11). A simple modified flow model with three parameters is presented to model the nonlinear behaviour (Karthigesu and Sri Ranjan, 1993). The simulated results of the five-percent bentonite and sand mixtures gave a better fit with the data when the equivalent diameter was selected in the range from 3.4E-05 m to 5.2E-05 m (Figures 5.7, 5.8 and 5.9). The simulated results of the ten-percent bentonite and sand mixtures have a better fit with the data than the Darcy's linear equation when the equivalent diameter was selected as 1.6E-05 m (Figure 5.10 and 5.11). A transitional hydraulic gradient value was chosen for each sample such that the simulated flow best fitted the data. In the model simulation, the viscosity of structured water was taken as ten and twenty times higher than that of free water for five-percent and ten-percent bentonite and sand samples, respectively. The hydraulic conductivity values at a hydraulic gradient value of one were compared with the

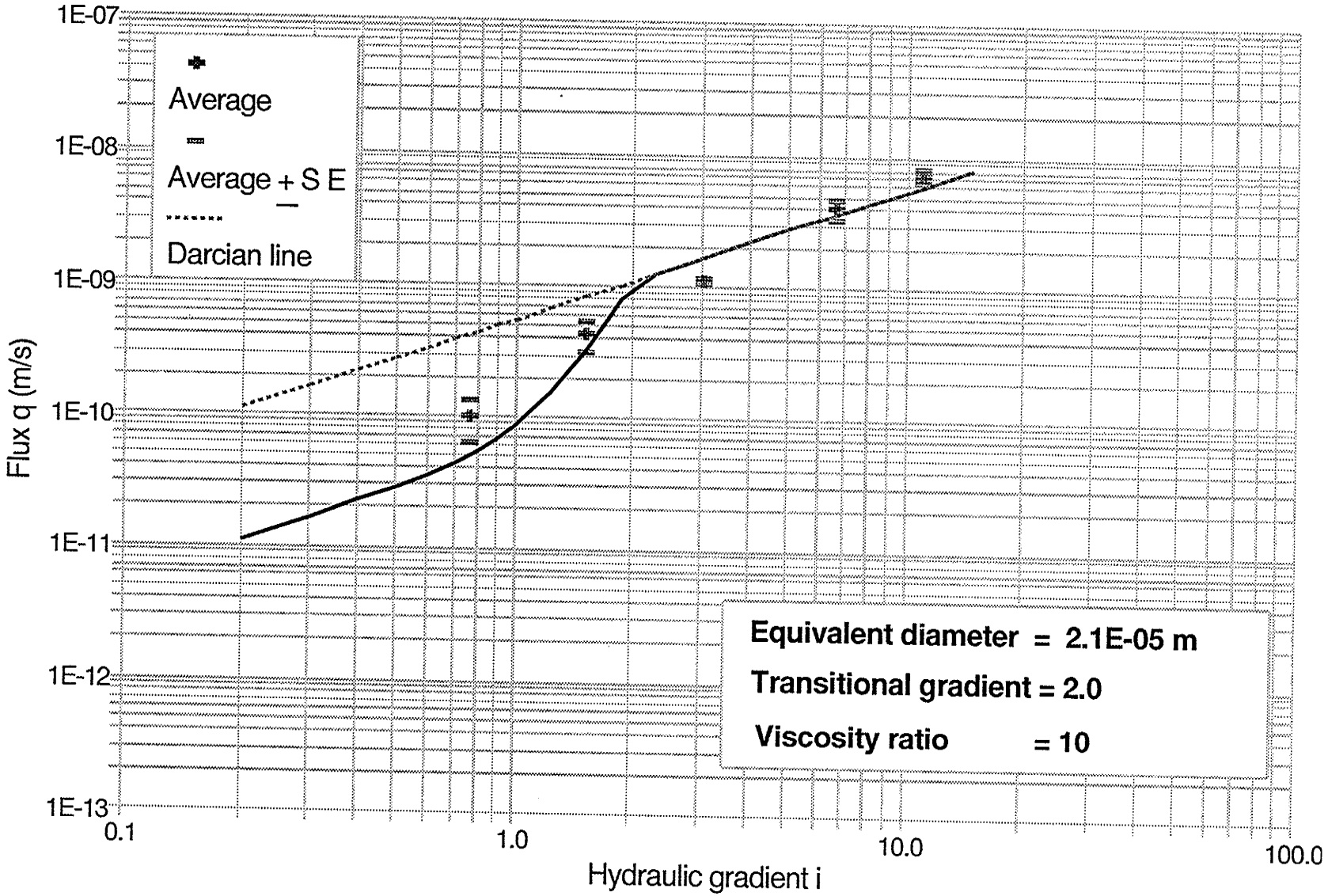

FIGURE 5.7 Modified flow model for 5P1

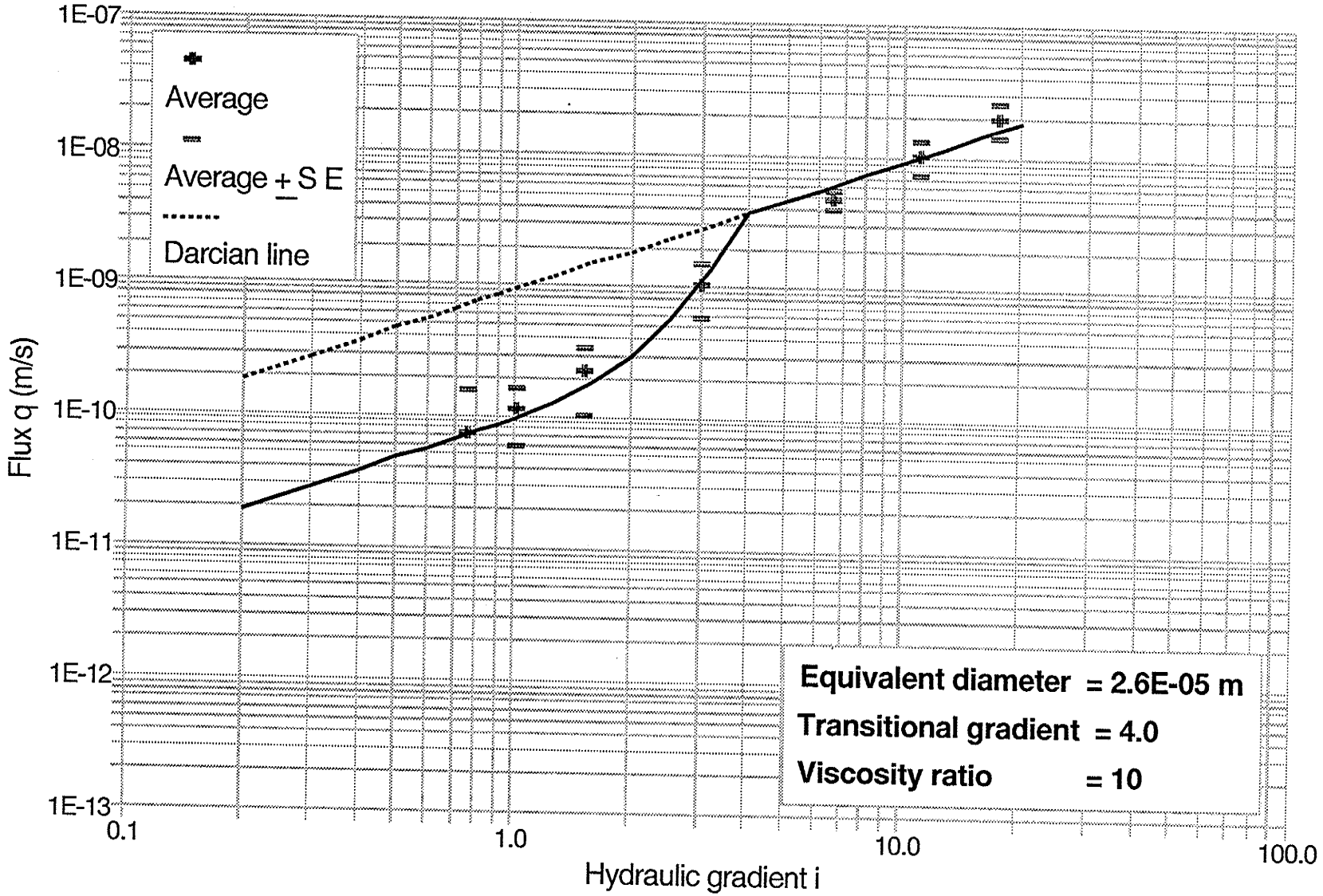

FIGURE 5.8 Modified flow model for 5P2

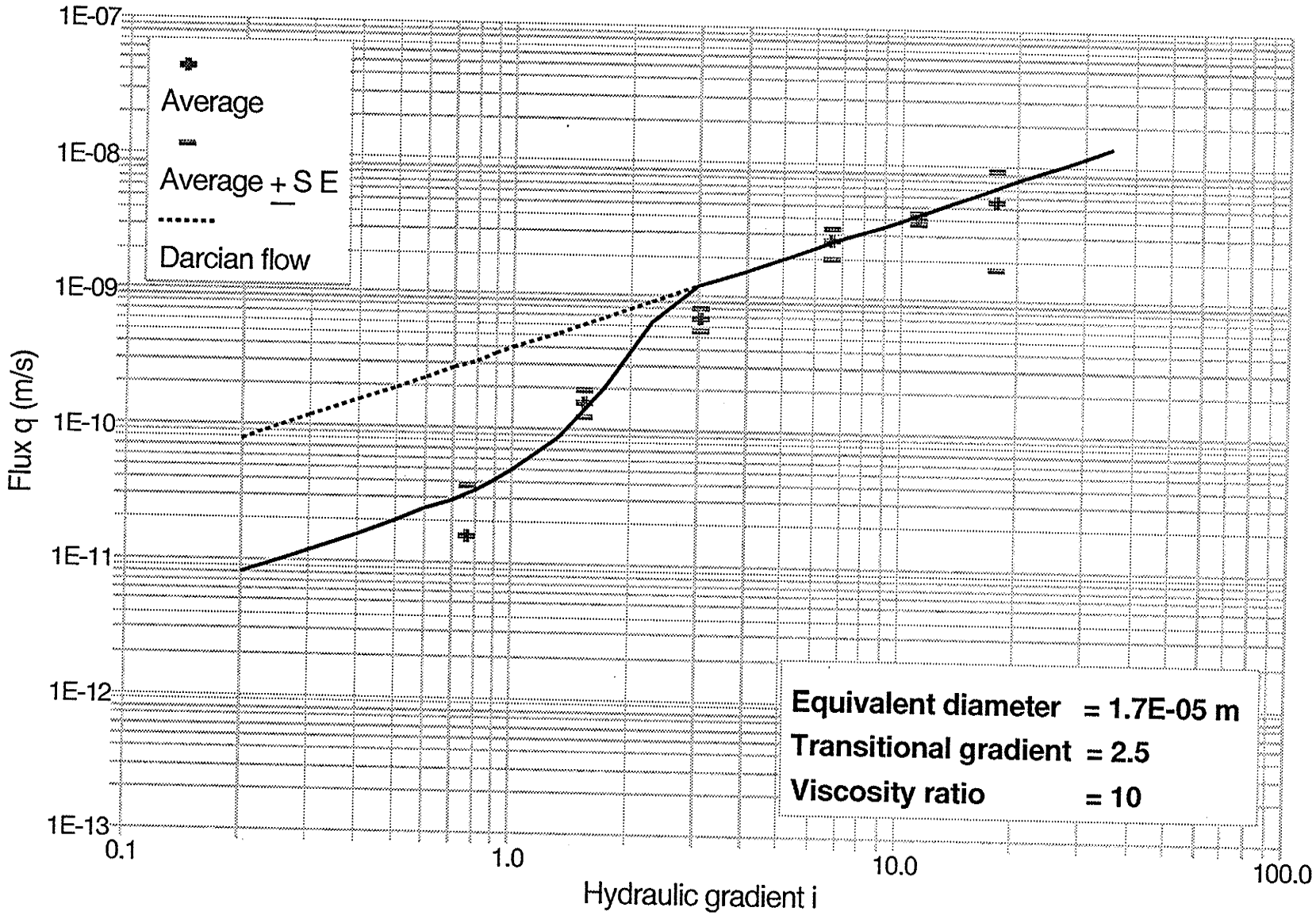

FIGURE 5.9 Modified flow model for 5P3

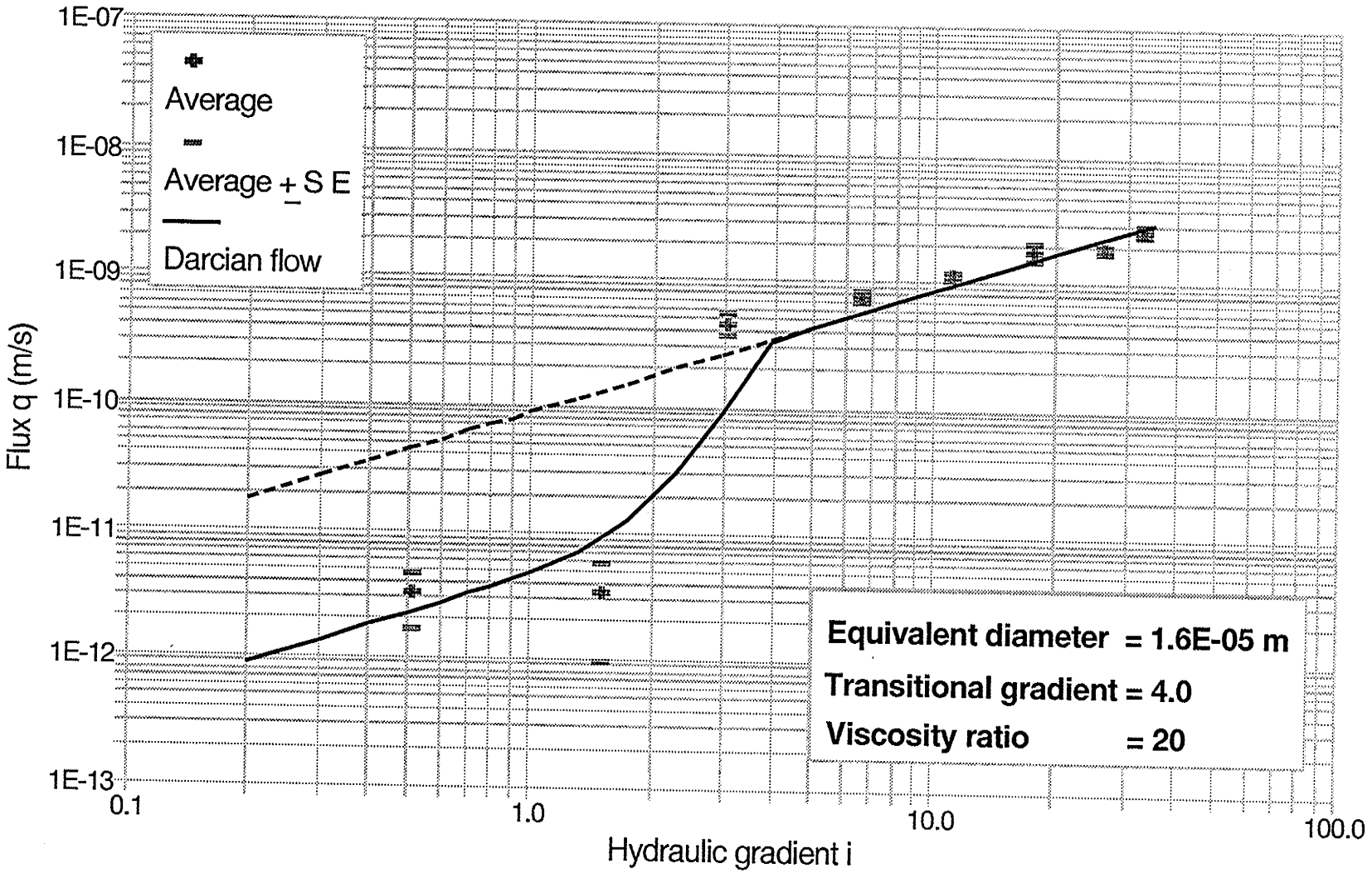

FIGURE 5.10 Modified flow model for 10P4

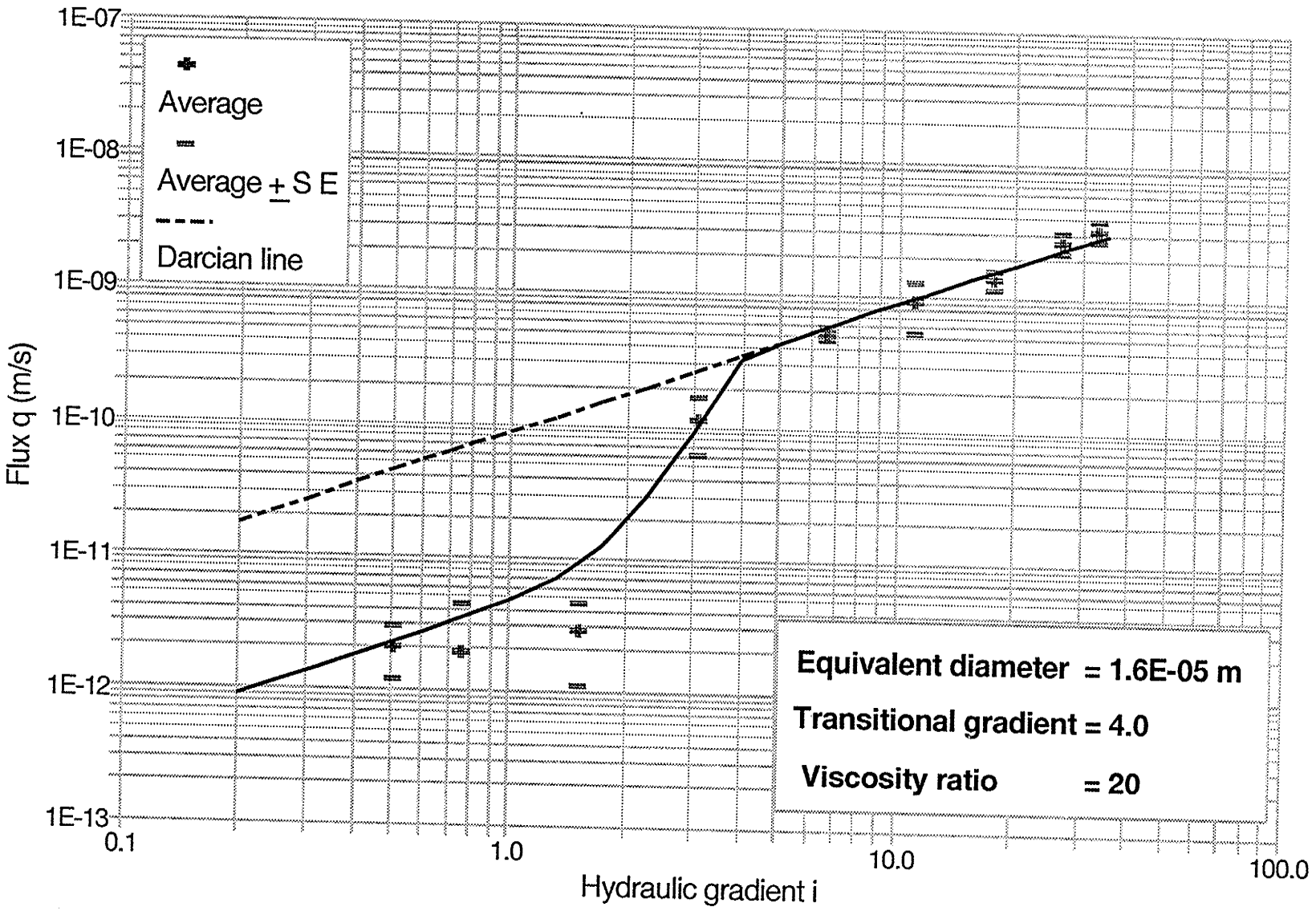

FIGURE 5.11 Modified flow model for 10P6

high-hydraulic-gradient-range hydraulic conductivity for the ten-percent and five-percent bentonite and sand samples in Table 5.1.

TABLE 5.1 Saturated hydraulic conductivity of five-percent and ten-percent samples of bentonite and sand in the low-hydraulic-gradient range and high-hydraulic-gradient range

Sample no.	Bentonite content	Hydraulic conductivity	
		At gradient = 1.0 (Model)	High gradient
	%	m s^{-1}	
5P1	5.0	6.0E-11	6.0E-10
5P2	5.0	1.0E-10	1.0E-09
5P3	5.0	4.0E-11	4.0E-10
10P4	10.0	4.0E-12	1.0E-10
10P6	10.0	4.0E-12	1.0E-10

5.3 Application of the Kozeny-Carman equation to the laboratory data

Equivalent diameters of the mixtures tested were calculated by substituting the measured high-hydraulic-gradient-range hydraulic conductivity values in Equation 3.28 which was derived from Kozeny-Carman equation. These values were compared with the values used in the simulation (Table 5.2).

In Equation 3.28, the following values were used to calculate the equivalent diameter.

fluid viscosity μ = 980 Pa s

fluid density ρ = 997 kg m^{-3}

gravity g = 9.8 m s^{-1}

dimensionless shape factor K_s = 2.5*

tortuosity T = 2.0*

porosity ϕ = 0.20*

*Values in the literature for similar materials (Corey, 1990)

TABLE 5.2 Equivalent diameters used in the model simulation (U) and equivalent diameters calculated by the equation derived from the Kozeny-Carman equation using measured hydraulic conductivity values (C)

Sample	Equivalent diameter used(U)	Equivalent diameter calculated(C)	Used /calculated (U/C)
	m	m	
5P1	4.20E-05	3.70E-05	1.14
5P2	5.20E-05	4.77E-05	1.09
5P3	3.40E-05	3.02E-05	1.13
10P4	1.60E-05	1.51E-05	1.06
10P6	1.60E-05	1.51E-05	1.06

In all the samples, calculated diameters were smaller than the diameters used in the simulation. In both the five-percent and ten-percent bentonite and sand samples, calculated diameters were close to the diameters used in the model predictions. Calculated and the equivalent diameters used for the five-percent bentonite and sand samples were two to three times larger than that of the corresponding diameters for the ten-percent bentonite and sand samples.

The ratio of viscosity of structured water to the viscosity of free water was chosen as 10 and 20 for five-percent and ten-percent samples respectively such that the modified flow lines fit the data best. The change in viscosity in relation to the type of clay and

distance from the clay surface is not clearly known at this time. A nuclear magnetic resonance (NMR) technique could be used to determine or estimate the viscosity of structured water as a function of distance from the clay surface at different imposed hydraulic gradients..

5.4 Summary

Based upon the limited laboratory results with five-percent and ten-percent bentonite and sand samples and using the model predictions, it appears that doubling the bentonite content from five-percent to ten-percent resulted in a one-order-of-magnitude reduction in hydraulic conductivity in the high-hydraulic-gradient range (Figure 5.12). The effective cross-sectional area of a sample depends on the number and size of capillaries that contribute to the flow at a given time. Darcy's law relates only to the macroscopic flux because of the imposed hydraulic gradient. Although the model simulation considered the differences at the capillary level, it does not take into account differences in the effective cross-sectional area or tortuosity of the capillaries. Better correlation could perhaps have been obtained by correcting it for tortuosity and effective cross-sectional area.

When measurements were complete, the samples were removed, filled with water in the outflow and inflow tubes, wrapped in an aluminum foil and kept for further testing. Tests that could be conducted later on these samples may show the effect, if any, of long-term storage on the hydraulic conductivity of this clay.

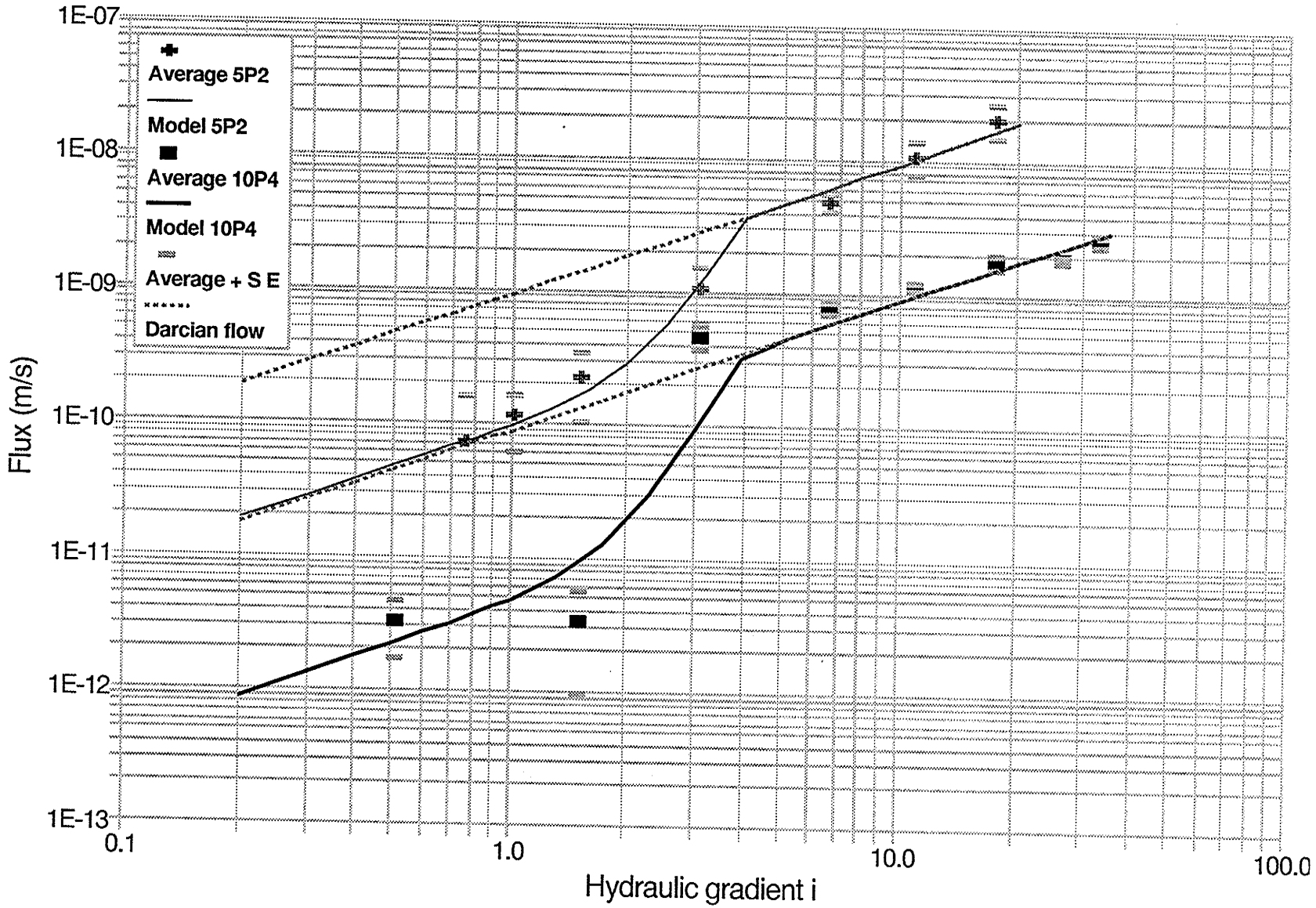

FIGURE 5.12 Flux versus hydraulic gradient - 5P2 and 10P4

The suggested model gives a possible explanation for the non-linear low-hydraulic-gradient flow behaviour. The use of hydraulic conductivity values obtained from samples, tested under higher hydraulic gradients may tend to over-estimate the flow rates under low hydraulic gradients. Different types of clays should be tested to generalize the low-hydraulic-gradient flow behaviour and to validate the proposed model. This is beyond the scope of my thesis work, but this could be examined in a future study.

6 Conclusion

Non-hydraulic mechanisms and their relative contribution were not considered in the studies conducted in the past. Effects of non-hydraulic mechanisms under low hydraulic gradients should be estimated to determine the relative importance of hydraulic flow under such conditions.

The flux as a function of hydraulic gradient in a log-log plot of five-percent and ten-percent bentonite and sand samples was characterized by a change in slope in the hydraulic gradient range from one to four. The hydraulic conductivity value in the lower range of hydraulic gradients was lower than the value obtained at the higher range of hydraulic gradients.

The five-percent bentonite and sand samples and the ten-percent bentonite and sand samples, except for 10P5, showed a gradient-dependent hydraulic conductivity below the transitional hydraulic gradient.

The proposed modified flow model uses three parameters, that is, equivalent diameter, transitional hydraulic gradient and viscosity ratio. Equivalent diameters calculated using the Kozeny-Carman equation closely matched the equivalent diameters used in the model simulation.

In the model simulation, the viscosity ratio of structured water to free water was chosen as 10 for the five-percent samples and 20 for the ten-percent samples. When the viscosity of structured water near the clay surfaces is more clearly known, these values could be refined in the model.

The macroscopic flow through the soil is the result of flow through several capillaries. The suggested model gives a possible explanation for the non-linear low-hydraulic-gradient flow behaviour. Different types of clays should be tested to generalize the low-hydraulic-gradient flow behaviour and to validate the proposed model.

7 Bibliography

Adam, N. K. 1941. The physics and chemistry of surfaces. Oxford University Press, London. pp. 180-188

Adam, K. M. 1967. Diffusion of entrapped gas from porous media. Ph. D. dissertation, Colorado State University, Fort Collins, CO. 129 pp.

Cherry, J. A., R. W. Gillham, and J. F. Barker. 1984. Contaminants in groundwater: chemical processes. In groundwater contamination. National Academy Press 3: 46-66

Craig, R. F. 1974. Soil mechanics. Van Nostrand Reinhold Company Ltd. pp. 26-27

Corey, A. T. 1990. Mechanics of immiscible fluids in porous media. Water resources publications, P. O. Box 2841, Littleton, CO. pp. 21-22

D'Arcy, H. 1856. Determination of the laws of the flow of water through sand (translated from the French). In Freeze. R. A. and W. Back. 1983. (Ed.). Physical Hydrogeology. Huchinson Ross, Troudsburg, PA. pp. 14-20

Dunn, R. J. and J. K. Mitchell. 1984. Fluid conductivity testing of fine grained soils. J. Geotech. Engrg. Div., ASCE 110: 1648-1665

Gillott, J. E. 1987. Clay in engineering geology : Developments in geotechnical Engineering. Vol. 41, Elsevier Science Publishers B. V., Amsterdam. pp. 285-297

Gödecke, H. J. 1980. Fliessgesetz für die Porenwasserdurchströmung feinkörniger Böden (Flow relationships for pore water permeation in fine-grained soils). Die Bautechnik 6: 184-193 (cited by Hoeks et al. 1987)

Grim, R. E. and N. Guven. 1978. Bentonites, geology, minerology, properties and uses - developments in sedimentology, 24, Elsevier, Amsterdam. pp. 217-248

Gupta, R. P. and D. Swartzendruber. 1962. Flow associated reduction in the hydraulic conductivity of quartz sand. Soil Sci. Soc. Am. J. 26: 6-10

Hansbo, S. 1960. Consolidation of clay with special reference to influence of vertical sand drains. Swed. Geotech. Inst. Proc., No 18, Stockholm. pp. 41-46

Hasenpatt, R., W. Degen, and G. Kahr. 1989. Flow and diffusion in clays. Appl. Clay Sci. 4: 179-192

Hoeks, J., H. Glas, J. Hofkamp, and A. H. Ryhiner. 1987. Bentonite liners for isolation of waste disposal sites. Waste Manag. Res. 5: 93-105

Karthigesu, T. and R. Sri Ranjan. 1992. Non-linear low gradient flow through sand bentonite mixtures. Paper No: 92-101, CSAE, Box 306 RPO, University of Saskatchewan, Saskatoon SK.

Karthigesu, T. and R. Sri Ranjan. 1993. Non-Darcy flow phenomena in sand bentonite mixtures. Paper No: 93-2002, Am. Soc. Ag. Eng., St. Joseph, MI.

Kemper, W. D. 1960. Water and ion movement in thin films as influenced by the electrostatic charge and diffuse layer of cations associated with clay mineral surfaces. Soil Sci. Soc. Am. J. 24: 10-16

Li, S. P. 1963. Measuring extremely low flow velocity of water in clays. Soil Sci. 95: 410-413

Low, P. F. 1961. Physical chemistry of clay water interaction. In Advances in Agronomy. Academic Press, Inc., New York 13: 269- 327

Low, P. F. 1976. Viscosity of interlayer water in montmorillonite. Soil Sci. Soc. Am. J. 40: 500-505

Low, P. F. 1979. Nature and properties of water in montmorillonite-water systems. Soil Sci. Soc. Am. J. 43: 651-658

Lutz, J. F. and W. D. Kemper. 1959. Intrinsic permeability of clays as affected by clay water interaction. Soil Sci. 88: 83-90

Martin, R. T. 1962. Adsorbed water on clay - a review. In clays and clay minerals. Pergamon Press Inc., New York. pp. 28-70

Miller, R. J. and P. F. Low. 1963. Threshold gradient for water flow in clay systems. Soil Sci. Soc. Am. J. 27: 605-609

Mitchell, J. K. and J. S. Younger. 1967. Abnormalities in hydraulic flow through fine-grained soils. In Permeability and Capillarity of Soils. ASTM STP 417. pp. 106-141

Olsen, H. W. 1965. Deviations from Darcy's law in saturated clays. Soil Sci. Soc. Am. J. 29: 135-140

Olsen, H. W. 1966. Darcy's law in saturated kaolinite. Water Resour. Res. 2: 287-295

Olsen, H. W. 1969. Simultaneous fluxes of liquid and charge through saturated kaolinite. Soil Sci. Soc. Am. J. 33: 338-344

Olsen, H. W. 1985. Osmosis: a cause of apparent deviations from Darcy's law. Can. Getech. J. 22: 238-241

Pickett, A. G. and M. M. Lemcoe. 1959. An investigation of shear strength of the clay-water system by radio-frequency spectroscopy. J. Geoph. Res. 64: 1579-1586

Ross, C. S. and E. V. Shannon. 1926. The minerals of bentonite and related clays and their physical properties. J. Amer. Ceram. Soc. 9: 77-96

Shackelford, C. D., D. E. Daniel, and H. M. Liljestrand. 1989. Diffusion of inorganic chemical species in compacted clay soil. J. Contam. Hydrol. 4: 241-273

Smith, W. O. and M. D. Crane. 1930. The Jamin effect in cylindrical tubes. J. Amer. Chem. Soc. 52: 1345-1349

Sri Ranjan, R. and R. W. Gillham. 1991. Non-linear electro-osmotic and hydraulic flow phenomena in saturated clays. Paper No: 91-105, CSAE, Box 306 RPO, University of Saskatchewan, Saskatoon SK

Sri Ranjan, R. and T. Karthigesu. 1992. Validity of conventional hydraulic conductivity measurement methods for clayey soils. 35th Annual meeting, Manitoba Society of Soil Science, January 6-7, Winnipeg MB. pp. 104-108

Swartzendruber, D. 1968. The applicability of Darcy's law. Soil Sci. 32: 11-18

Tavenas, F., P. Leblond, P. Jean, and S. Lerouli. 1983. The permeability of natural soft clays. Part I: Methods of laboratory measurement. Can. Geotech. J. 20: 629- 644

Von Englehardt, W. and W. L. M. Tunn. 1955. The flow of fluids through sandstones. Illinois State Geol. Surv. Circ.194. pp. 1-17

Van Olphen, H. 1963. An introduction to clay colloid chemistry. John Wiley & Sons, New York. pp. 130-137

Wang, M. C. and C. C. Huang. 1984. Soil compaction and permeability prediction models. J. Envir. Eng. 10: 1063-1083

Appendix I

```
C       MODIFIED TWO LAYER VISCOUS SATURATED FLOW IN
C       BENTONITE-SAND MIXTURES UNDER LOW HYDRAULIC GRADIENTS

      PARAMETER(NN=100)
      DOUBLE PRECISION R0,V1,V2,R1(NN),FLUX(NN),GRAD(NN),THG,K(NN)
      DOUBLE PRECISION DTS,DTL,GMAX,VR,ED
      INTEGER I,N1
      OPEN (UNIT=9,FILE='B:BEN-DT')
      WRITE(*,*)'ENTER THE INCREMENT IN HYDRAULIC GRADIENT VALUE'
      WRITE(*,*)'FOR THE LOW-HYDRAULIC-GRADIENT RANGE'
C       SMALL INCREMENTAL VALUE WILL GIVE A SMOOTH CURVE WHEN FLUX
C       IS PLOTTED AGAINST THE HYDRAULIC GRADIENT. THIS INCREMENT IS
C       USED UPTO TRANSITIONAL HYDRAULIC GRADIENT
      READ(*,*)DTS
      WRITE(*,*)'ENTER THE INCREMENT IN HYDRAULIC GRADIENT VALUE'
      WRITE(*,*)'FOR THE HIGH-HYDRAULIC-GRADIENT RANGE'
      READ(*,*)DTL
      WRITE(*,*)'ENTER THE VALUE OF MAXIMUM HYDRAULIC GRADIENT'
      READ(*,*)GMAX
      WRITE(*,*)'ENTER THE EQUIVALENT DIAMETER'
      READ(*,*)ED
      WRITE(*,*)'ENTER THE TRANSITIONAL HYDRAULIC GRADIENT'
      READ(*,*)THG

C       THG=4.
C       DTS=0.1
C       DTL=1
C       ED = 5.2E-05

C       R0 - Equivalent radius in m
C       ED - Equivalent diameter in m
C       V1 - Viscosity of water
C       V2 - Viscosity of Structured water
C       VR - Viscosity ratio
C       THG - Transitional hydraulic gradient


      R0=ED/2.0
      N1=INT(THG/DTS)
      NF=INT(THG/DTS) + INT ((GMAX - THG)/DTL)
      VR=10.0
      V1=890.0
      V2=V1*VR

      DO 10 I=1,N1
        GRAD(I)=I*DTS
        R1(I)=R0/THG*GRAD(I)
        IF ( R1(I).GT.R0) R1(I)=R0
10    CONTINUE

      DO 30 I=N1+1,NF
        GRAD(I)=GRAD(N1)+(I-N1)*DTL
        R1(I)=R0/THG*GRAD(I)
        IF ( R1(I).GT.R0) R1(I)=R0
30    CONTINUE

      DO 40 I=1,NF
C -----------------K  Below Transitional hydraulic gradient ----------
```

```
         IF (GRAD(I) .GT. THG) GOTO 35
         K(I)=(997.0 * 9.8 * R0**2/ 8.0)*(((1 - (GRAD(I)/THG) ** 4)/V2)
     +   + ( ((GRAD(I)/THG) ** 4)/V1))
       GOTO 36
C ----------------K  above Transitional hydraulic gradient ----------

 35      K(I)= (997.0 * 9.8 * R0**2 /(V1 * 8.0))
 36      FLUX(I) = K(I) * GRAD(I)
 40    CONTINUE


C------------------ Output ----------------------------------------
      WRITE(*,*) 'Parametric values used in the simulation'
      WRITE(*,*) ED
      WRITE(*,60) ED
      WRITE(*,70) THG
      WRITE(*,80) VR
      WRITE(*,*)

      WRITE(9,*) 'Parametric values used in the simulation'
      WRITE(9,*)
      WRITE(9,60) ED
      WRITE(9,70) THG
      WRITE(9,80) VR
      WRITE(9,*)

 60   FORMAT('Equivalent diameter                - ',E8.2)
 70   FORMAT('Transitional hydraulic gradient  - ',F8.2)
 80   FORMAT('Viscosity ratio                    - ',F8.2)

      WRITE(*,*) 'Gradient        Flux       Hydraulic conductivity'
      WRITE(*,*) '                 m/s                  m/s         '
      WRITE(9,*) 'Gradient        Flux       Hydraulic conductivity'
      WRITE(9,*) '                 m/s                  m/s         '

      DO 100 I=1,NF
         WRITE(*,200) GRAD(I),FLUX(I),K(I)
         WRITE(9,200) GRAD(I),FLUX(I),K(I)
200   FORMAT(F6.2,6x,2(E10.4,10x))
100   CONTINUE
      CLOSE(UNIT=9)
      END
```

Sample output file - BEN-DT

Parametric values used in the simulation

Equivalent diameter	-	0.52E-04
Transitional hydraulic gradient	-	4.00
Viscosity ratio	-	10.00

Gradient	Flux m/s	Hydraulic conductivity m/s
0.10	0.9277E-11	0.9277E-10
0.20	0.1855E-10	0.9277E-10
0.30	0.2784E-10	0.9279E-10
0.40	0.3714E-10	0.9285E-10
0.50	0.4648E-10	0.9297E-10
0.60	0.5591E-10	0.9319E-10
0.70	0.6548E-10	0.9355E-10
0.80	0.7528E-10	0.9410E-10
0.90	0.8541E-10	0.9491E-10
1.00	0.9603E-10	0.9603E-10
1.10	0.1073E-09	0.9754E-10
1.20	0.1194E-09	0.9953E-10
1.30	0.1327E-09	0.1021E-09
1.40	0.1474E-09	0.1053E-09
1.50	0.1639E-09	0.1093E-09
1.60	0.1826E-09	0.1141E-09
1.70	0.2040E-09	0.1200E-09
1.80	0.2286E-09	0.1270E-09
1.90	0.2570E-09	0.1353E-09
2.00	0.2899E-09	0.1449E-09
2.10	0.3280E-09	0.1562E-09
2.20	0.3722E-09	0.1692E-09
2.30	0.4233E-09	0.1840E-09
2.40	0.4823E-09	0.2010E-09
2.50	0.5504E-09	0.2202E-09
2.60	0.6287E-09	0.2418E-09
2.70	0.7184E-09	0.2661E-09
2.80	0.8210E-09	0.2932E-09
2.90	0.9380E-09	0.3234E-09
3.00	0.1071E-08	0.3569E-09
3.10	0.1221E-08	0.3940E-09
3.20	0.1391E-08	0.4347E-09
3.30	0.1582E-08	0.4795E-09
3.40	0.1797E-08	0.5286E-09
3.50	0.2038E-08	0.5822E-09
3.60	0.2306E-08	0.6405E-09
3.70	0.2605E-08	0.7040E-09
3.80	0.2937E-08	0.7728E-09
3.90	0.3304E-08	0.8472E-09
4.00	0.3711E-08	0.9277E-09
5.00	0.4638E-08	0.9277E-09
6.00	0.5566E-08	0.9277E-09
7.00	0.6494E-08	0.9277E-09
8.00	0.7421E-08	0.9277E-09
9.00	0.8349E-08	0.9277E-09
10.00	0.9277E-08	0.9277E-09
11.00	0.1020E-07	0.9277E-09
12.00	0.1113E-07	0.9277E-09
13.00	0.1206E-07	0.9277E-09
14.00	0.1299E-07	0.9277E-09

15.00	0.1391E-07	0.9277E-09
16.00	0.1484E-07	0.9277E-09
17.00	0.1577E-07	0.9277E-09
18.00	0.1670E-07	0.9277E-09
19.00	0.1763E-07	0.9277E-09
20.00	0.1855E-07	0.9277E-09
21.00	0.1948E-07	0.9277E-09
22.00	0.2041E-07	0.9277E-09
23.00	0.2134E-07	0.9277E-09
24.00	0.2226E-07	0.9277E-09
25.00	0.2319E-07	0.9277E-09
26.00	0.2412E-07	0.9277E-09
27.00	0.2505E-07	0.9277E-09
28.00	0.2597E-07	0.9277E-09
29.00	0.2690E-07	0.9277E-09
30.00	0.2783E-07	0.9277E-09